iScience

CellPress
OPEN ACCESS

Article

Adult neurogenesis in crayfish: Identity and regulation of neural progenitors produced by the immune system

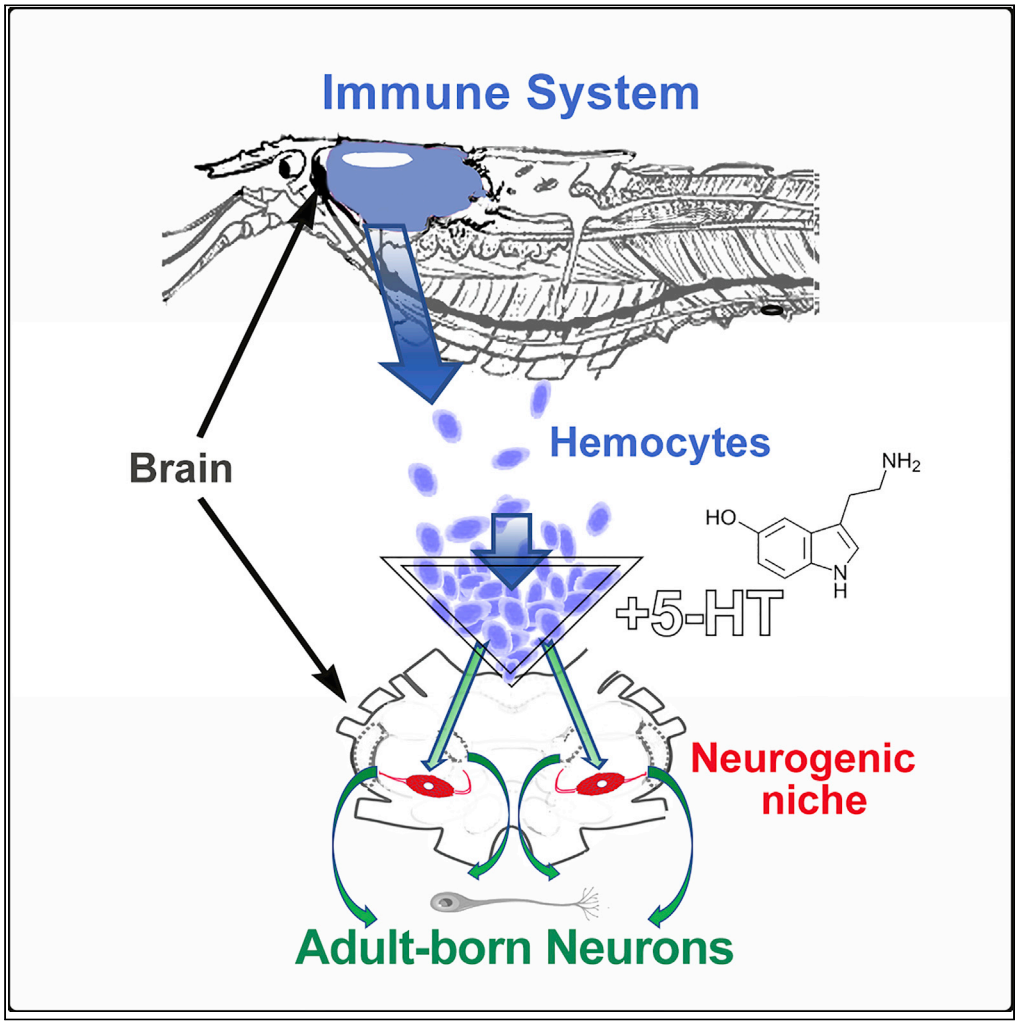

Jeanne L. Benton, Emmy Li, Emily Weisbach, ..., Paula Grazielle Chaves da Silva, Alex J. Edwards, Barbara S. Beltz

bbeltz@wellesley.edu

Highlights

The dynamics of cell proliferation and release from the APC and HPT are distinct

Hyaline cells, but no other hemocyte types, proliferate *in vivo* and *in vitro*

5-HT and the cytokine AST1 coordinate the immune response and adult neurogenesis

Hyaline hemocytes are the prime neural progenitor cell candidates

Benton et al., iScience *25*, 103993
April 15, 2022
https://doi.org/10.1016/j.isci.2022.103993

iScience

CellPress
OPEN ACCESS

Article

Adult neurogenesis in crayfish: Identity and regulation of neural progenitors produced by the immune system

Jeanne L. Benton,[1] Emmy Li,[1,2] Emily Weisbach,[1,3] Yuriko Fukumura,[1] Virginia C. Quinan,[1] Paula Grazielle Chaves da Silva,[1] Alex J. Edwards,[1] and Barbara S. Beltz[1,4,*]

SUMMARY

Adult-born neurons are incorporated into brain circuits in the crayfish *Procambarus clarkii*, as in many vertebrate and invertebrate species. Adult neurogenesis depends on several conserved features, including the presence of neurogenic niches housing progenitor cells and the expansion, migration, and differentiation of their daughters, the neural precursor cells. However, in contrast to mammalian species, the progenitors initiating the neurogenic lineage in *P. clarkii* do not undergo long-term self-renewal. A central question is the mode of replenishment of these cells. Experiments have shown that hemocytes generated by the immune system, and not other cell types, are attracted to and incorporated into the niche. The present studies highlight the interdependency of the immune and nervous systems in the generation of adult-born neurons, by demonstrating that hyaline hemocytes are the probable neural progenitor cells, and that serotonin and the cytokine astakine 1 regulate both immune function and adult neurogenesis.

INTRODUCTION

New neurons are born and incorporated into circuits in the adult brains of many vertebrate and invertebrate organisms. In decapod crustaceans, new neurons are added to visual areas, as well as to two groups of brain cells (Clusters 9 and 10) containing local and projection neurons that innervate the olfactory and accessory lobe pathways (Beltz and Benton, 2017).

The cellular lineage producing the adult-born neurons in Clusters 9 and 10 has been identified in *Procambarus clarkii* (Sullivan et al., 2007; Song et al., 2009; Brenneis and Beltz, 2020). The bipolar neural progenitors reside in a neurogenic niche located on the ventral surface of the brain that is closely associated with the vasculature (Figure 1A); each progenitor cell has a short process that extends to a vascular cavity in the niche, and a long process that extends to either Cluster 9 or 10 (Sullivan et al., 2007). Unlike traditional stem cells, however, these progenitors do not undergo long-term self-renewal, as there is no evidence for retention of proliferation markers (e.g., 5-bromo-2′-deoxyuridine, BrdU; 5-ethynyl-2′-deoxyuridine, EdU) in the niche (Benton et al., 2011, 2013). The progenitor cells, which divide infrequently, undergo symmetrical divisions when they are positioned adjacent to the vascular cavity (Brenneis and Beltz, 2020). Daughters of these divisions subsequently undergo several slightly asymmetric divisions, and these clones along with their mother cells migrate along fibrous streams formed by the long processes of niche progenitor cells (Brenneis and Beltz, 2020). Once these cells reach proliferation zones in Cluster 9 or 10, they divide again before differentiating into neurons (Sullivan and Beltz, 2005; Kim et al., 2014).

Although the niche progenitor cells in *P. clarkii* do not undergo long-term self-renewal, these cells (~300 in adults) are never depleted and neurons continue to be generated throughout the relatively long lives (up to ~9 years; Scalici et al., 2010; Chucholl, 2011) of these animals (Zhang et al., 2009). We therefore concluded that the niche is not a closed system; the pool of neural progenitors must be replenished from an extrinsic source (Benton et al., 2011). Such an extrinsic source was confirmed by experiments in which crayfish received a single injection of BrdU, and the presence of BrdU-labeled cells in the niche was observed over a three-week period; these studies showed two BrdU labeling peaks, the first associated with intrinsic cells labeled in the niche at the time of BrdU injection. Following a "gap" of a few days when no labeled cells were observed in the niche, the second peak of BrdU-labeled niche cells occurred, several

[1]Neuroscience Department, Wellesley College, Wellesley, MA 02481, USA

[2]Biomedical Sciences Graduate Program, University of California, San Francisco, CA 94158, USA

[3]Rhode Island Hospital, 593 Eddy Street, Providence, RI 02903, USA

[4]Lead contact

*Correspondence: bbeltz@wellesley.edu

https://doi.org/10.1016/j.isci.2022.103993

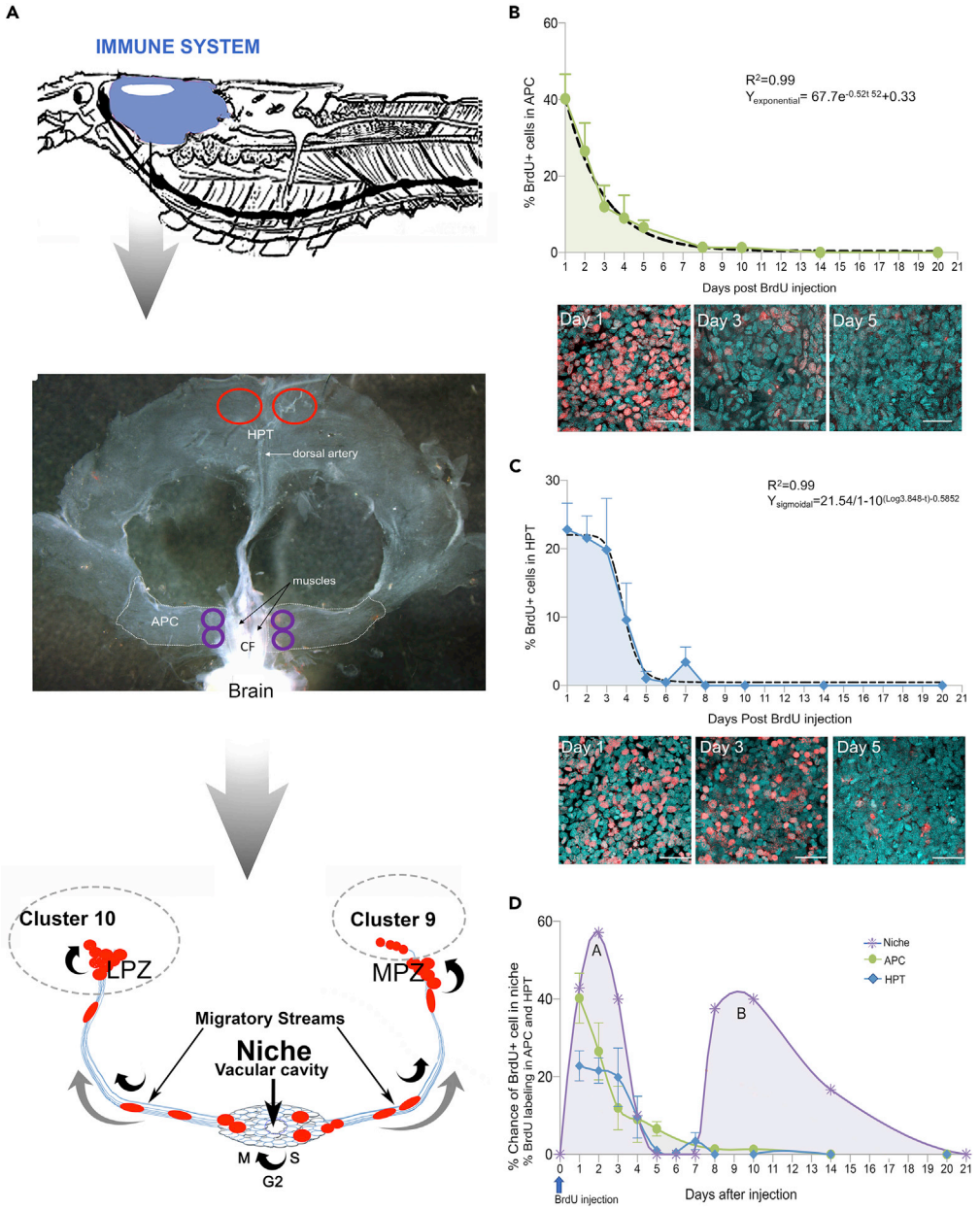

Figure 1. Cellular dynamics in the immune system tissues are compared

An injection of BrdU was given to a group of crayfish on day 0 and animals euthanized on the days specified in the graphs. Average percentages of BrdU-labeled APC (B) and HPT (C) cells and standard deviations are shown (B, C, D).

(A) (Top) The immune system (blue) is located in the anterior, dorsal region of crayfish, surrounding the stomach. (Middle) Illustration of dissected tissue regions and sampling sites in the two parts of the hematopoietic system: the APC and HPT. The APC is located just posterior to the brain, surrounding and extending away from the cor frontale (CF). In the APC, four images were taken per animal, bilaterally at regions adjacent to the muscles of the CF (locations circled in purple). In the HPT, which is located posterior to the APC, two images were taken per animal (locations circled in red) at the posterior margin of the HPT, adjacent to the dorsal artery. (Bottom) Neurogenic niches that generate adult-born neurons are located bilaterally on the ventral surface of the brain, just beneath the sheath that surrounds the brain. One niche is represented diagrammatically, illustrating the position of the niche and migratory streams, and locations of some of the mitotic divisions in the neural lineage (curved black arrows). The direction of movement of the neural precursors in the migratory streams, toward brain Clusters 9 and 10, is indicated (grey arrows).

(B) An average of 40% of APC cells in the sampled regions were BrdU-positive on day 1. The mean percentage of BrdU-labeled cells in the APC (green-shaded graph area) then decreased exponentially (dashed regression line) over the next

Figure 1. *Continued*
several days, reaching zero by 14 days post-injection. Confocal images are representative of APC labeling on days 1, 3, and 5. Propidium iodide (cyan); BrdU (red). *N* = # crayfish, each with multiple counting areas in each animal (see Methods): sampling days 1–2, *n* = 8; day 3, *n* = 6; day 4, *n* = 5; day 5, *n* = 6; day 8, *n* = 3; day 10, *n* = 4; day 14, *n* = 4; day 21, *n* = 4. R^2 and *Y* exponential functions are indicated. Error bars indicate standard deviations.
(C) In the HPT, the average percentage of BrdU-labeled cells remains at ~20% for the first three sampling days following BrdU injection, then falls to near zero between days 3 and 5. The dashed line represents a sigmoidal decay, which best fits these data. Images show BrdU labeling on days 1, 3, and 5 post-BrdU injection. Propidium iodide (cyan) and BrdU (red). *N* = # crayfish, with multiple counting areas in each animal (see Methods): sampling day 1, *n* = 5; day 2, *n* = 4; day 3, *n* = 3; day 4, *n* = 5; day 5, *n* = 4; day 6, *n* = 5; day 7, *n* = 6; day 8, *n* = 2; day 10, *n* = 2; day 14, *n* = 3; day 20, *n* = 4. R^2 and *Y* exponential functions are indicated. Error bars indicate standard deviations.
(D) The % chance of finding a BrdU-labeled cell in the neurogenic niche after a single injection of BrdU on day 0 is plotted (purple shaded graph; adapted from Benton et al., 2014). The proliferation dynamics (% BrdU-labeling) in the APC (green; shown also in Figure 1B) and HPT (blue; shown also in Figure 1C) are overlaid on the niche graph. Two separate groups of animals were used to generate the niche graph (purple), and APC/HPT graphs (green and blue). BrdU-labeled cells are found in the niche (purple) on days 1–4 (peak A) and again on days 8–14 post-BrdU injection (see Benton et al., 2014 for details). The % of BrdU-labeled cells in the APC and HPT decreases as cells from these tissues are released into the circulation. Scale bars: (B) and (C) 30 μm.

days after the BrdU clearing time; therefore, newly labeled cells could not explain this delayed peak. We came to the conclusion that cells labeled in the source tissue – and later released and incorporated into the niche – were responsible for this later peak in labeled cells (Benton et al., 2014).

In vitro (Benton et al., 2011) and *in vivo* (Benton et al., 2014) studies have demonstrated that cells extracted from the hemolymph (blood), but not other cell types, are attracted to the niche. Following the adoptive transfer of EdU-labeled hemocytes from donor to recipient crayfish, EdU-labeled cells can be found in the niche by day 3 following transfer; by seven weeks after transfer, labeled cells in Clusters 9 and 10 express transmitters appropriate for neurons in these cell clusters (Benton et al., 2014). Because circulating hemocytes originate in hematopoietic tissues, we concluded that the niche cells are replenished by the immune system (Benton et al., 2014).

In the experiments reported here, the immune source of neural progenitor cells was further tested by experiments in which recombinant-astakine 1 (r-AST1; gift of Irene Söderhäll, Uppsala University, Sweden), a crustacean prokineticin-family cytokine (Söderhäll et al., 2005), was injected into crayfish along with BrdU. AST1 promotes the differentiation and release of hemocytes from the immune system in *P. clarkii* (Benton et al., 2014), as in *Pacifascticus leniusculus* (Lin et al., 2010). We therefore hypothesized that AST1 would advance the late-appearing second peak of BrdU-labeled cells observed in the niche following a single injection of BrdU into crayfish. Indeed, following the injection of r-AST1, the gap in BrdU labeling of niche cells observed previously was completely obliterated by the premature release of cells from the anterior proliferation center (APC) and posterior hematopoietic tissue (HPT).

Another aim of these studies was to identify the specific type of circulating cell that becomes the neural progenitor. Three hemocyte types have been characterized in the blood of crayfish and related decapod crustaceans: granular, semigranular, and hyaline cells (Söderhäll, 2016). Adoptive transfer of specific hemocyte classes, separated with Percoll gradients, tested which cell type is most likely to incorporate into the niche. We find that only cells from the layer containing hyaline and semigranular hemocytes are incorporated into the niche, and these express appropriate neurotransmitters six weeks after transfer. In addition, short-term *in vitro* and *in vivo* studies indicate that hyaline cells are the only hemocyte type that is actively in the cell cycle and able to incorporate proliferation markers. Together, these data suggest that hyaline cells are the most likely neural progenitor cells.

A final goal of the current studies was to identify variables that influence the integration of adoptively transferred hemocytes into the niche, in order to determine whether the replenishment of the niche population is regulated. Adoptive transfers of EdU-labeled hemocytes from donors to naive recipients have been previously described (Benton et al., 2014); further studies showed that the incorporation rate for adoptively transferred hemocytes into the niche can be very low (Brenneis and Beltz, 2020). We therefore asked whether the magnitude of hemocyte incorporation into the niche varies depending on experimental conditions. Using a variation of previous adoptive transfer methods, recipient crayfish were treated with serotonin (5-hydroxytryptamine, 5-HT) after hemocyte transfer; 5-HT has been implicated as an attractant for

hemocytes to the niche (Benton et al., 2011). Raising 5-HT levels increased hemocyte integration into the niche following adoptive transfers, indicating that the low incorporation in earlier studies may have resulted from experimental variables that can be controlled and modulated.

Overall, these data (1) confirm the immune origin of progenitor cells responsible for adult neurogenesis in the crayfish brain, (2) identify hyaline hemocytes as the most likely neural progenitor cells, and (3) indicate that hormonal variations (e.g., circadian, seasonal, or in response to physiological stimuli) and environmental conditions that alter the composition of the hemolymph or hemocyte numbers, modulate the rate of hemocyte incorporation into the niche.

RESULTS AND DISCUSSION

Previously published studies examined the presence or absence of labeled cells in the neurogenic niche at intervals following a single injection of BrdU (Benton et al., 2014). These data revealed two peaks in BrdU labeling in the niche (Figure 1D) separated by a gap when no labeled cells were observed. The timing of the first peak was consistent with the clearing time for BrdU (~36–48 h; Benton et al., 2011), the cell cycle time of the niche cells (~48 h), and the limited self-renewal capacity of the niche cells (Benton et al., 2013). Surprisingly, however, an extended second peak in BrdU labeling was observed in the niche after the gap period. This delayed peak has been attributed to the labeling of neural progenitors in their source tissue, followed by their release, maturation, and incorporation into the niche. These findings prompted a number of questions; paramount among these is to confirm the source tissue of the neural progenitors. Previous experiments suggested this source is the immune system (Benton et al., 2011, 2014). The goals of the present studies were to further test the immune system's role in the generation of neurons by identifying the specific hemocyte type that replenishes the progenitor pool and by testing whether immune system modulators (i.e., AST1 and 5-HT) also influence neurogenesis.

Cellular dynamics in the immune system tissues are compared (Figure 1)

Following a single pulse of BrdU, proliferating cells were tracked in the two regions comprising the immune system (APC and HPT; Söderhäll, 2016) (Figures 1B and 1C). The APC and more posterior HPT are contiguous tissues located on the dorsal side of the gut, surrounding the dorsal artery; the APC surrounds the cor frontale (Figure 1A) adjacent to the brain, and contains a highly proliferative and largely undifferentiated population of cells containing loose euchromatin, suggesting this may be a stem cell region. In contrast, the posterior HPT contains four to five cell types containing dense heterochromatin, organized in repeating lobules (Noonin et al., 2012). Our hypothesis in the current experiments was that the dynamics of BrdU labeling in these tissues and their response to AST1 might implicate one of these areas as the source of neural precursors in the niche.

The APC: the percentage of BrdU-labeled cells decreases exponentially

The percentage of BrdU-labeled cells in immune tissues (APC, HPT) was examined at intervals after BrdU injection (Figures 1B and 1C), following the timing protocol used previously to examine BrdU labeling of neural precursor cells in the niche (Figure 1D; shaded graph adapted from Benton et al., 2014). Four readily identifiable proliferative regions in the APC were assessed in order to ensure repeatability of the analysis; these same regions were analyzed in earlier APC studies (Chaves da Silva et al., 2013). In the current experiments, these regions also serve as assays for the influence of AST1 on the APC.

In the APC, ~40% of all cells were consistently labeled 1 day after BrdU injection (Figure 1B), in agreement with previous studies (Chaves da Silva et al., 2013). An exponential decline in labeled cells (R^2 = 0.99) was then observed over the next 10 days, until the percentage of BrdU-labeled cells decreased to zero by day 14 (Figure 1B). This rapid incorporation of BrdU and precipitous decline in labeled cells suggests that the APC contains a highly proliferative population of cells that are being quickly released into the circulation.

Cellular dynamics in the HPT contrast with cells in the APC

The posterior HPT was sampled on either side of the dorsal artery (Figure 1A). Cells in these regions display BrdU-labeling dynamics that are distinct from the APC (Figure 1C). For the first three sampling days following BrdU injection, the percentage of BrdU-labeled cells stabilizes between 20 and 25%, consistent with findings in other species (Söderhäll et al., 2003). The initial degree of labeling is therefore roughly half of what is observed in the APC, suggesting very different cell cycle times (and/or length of S phase) in these

tissues. However, the percentage of BrdU-labeled cells falls to near zero between days 3 and 5, reaching this point more rapidly than in the APC. Therefore, despite being anatomically connected as one tissue (Chaves da Silva et al., 2013; Noonin et al., 2012), the cellular dynamics of the APC and HPT are very different. To provide temporal context, the APC and HPT graphs are superimposed on the previously published graph of BrdU labeling in the niche following a single injection of BrdU (Figure 1D; Benton et al., 2014).

The dynamics of cell labeling with proliferation markers in the APC and HPT are therefore distinct. Many previous studies have demonstrated the release of hemocytes from crustacean hematopoietic tissues into the vascular system (see the review in Söderhäll, 2016), and there is currently no evidence for movement of cells within or between the APC and HPT (Benton and Beltz, unpublished results). Accordingly, the rapid decline in BrdU labeling observed in these regions is interpreted as the release of cells into the circulation. Current research is therefore examining in detail the circulating hemocyte population, including quantitative studies of the three different hemocyte types in *P. clarkii*.

AST1 alters cellular dynamics in the niche and immune system (Figures 2 and 3)

The cytokine AST1, a member of the prokineticin family, promotes the maturation and release of hemocytes from hematopoietic tissues in *Pacifastacus leniusculus* (Söderhäll et al., 2005; Söderhäll, 2016). An increase in semigranular hemocytes is primarily responsible for the large increase in total hemocyte count (THC) following injection of the recombinant form of AST1 (r-AST1; Lin et al., 2010). Likewise, injection of *P. clarkii* with r-AST1 results in a ~70% increase in THC at 12 h after injection (Benton et al., 2014), although the specific hemocyte type(s) responsible for this increase is not known.

In order to further test the relationship between the immune and nervous systems, we introduced r-AST1 along with BrdU and repeated the sampling protocol used to generate the APC, HPT, and niche graphs in Figure 1D. These experiments tested the hypotheses that AST1 will advance the late-appearing BrdU-labeled cells in the niche (peak B in graph 1D) owing to the premature release of cells from the hematopoietic system, and that the APC and HPT will have distinct responses to AST1.

AST1 alters the arrival-time of BrdU-labeled cells in the neurogenic niche

Following a simultaneous injection of BrdU and r-AST1 on day 0, BrdU-labeled cells were quantified in the niches of crayfish that were sacrificed daily for one week after BrdU injection and at intervals thereafter for 21 days, following the same schedule as in previous studies (Benton et al., 2014). The probability of observing BrdU-labeled cells in the niche was then plotted for each of the sampling days (Figure 2A, red dashed line). The actual counts of BrdU-labeled niche cells are superimposed on the probability graph in Figure 2B.

BrdU-labeled cells are present in the niche at all sampled time points, with four distinct peaks on days 2, 4, 7 ,and 10 post-injection (peaks C–F, Figure 2A). This contrasts with the two peaks (A and B) observed in earlier studies without AST1. We conclude that peak C represents the labeling of intrinsic cells in the niche with BrdU (as does peak A, Figure 2A). Peak D is of special interest, as this occurs on day 4, when the initial number of labeled niche cells was rapidly declining during the BrdU-only experiment (Benton et al., 2014) (see overlay, Figure 2A). Whereas there was only a 10% chance of finding labeled cells in the niche on day 4 in the BrdU-only protocol, r-AST1 injections along with BrdU increased the chance of finding BrdU-labeled cells in the niche to 50%. Previous experiments have shown that r-AST1 injection into crayfish results in increased incorporation of BrdU by, and increased the number of, niche cells (Benton et al., 2014), indicating that AST1 promotes the proliferation of these cells. Peak D may therefore reflect a higher rate of proliferation in cells intrinsic to the niche, which is consistent with the doubling in the average number of labeled niche cells in the histogram (Figure 2B).

Peak E appears during the "gap" period defined in previous BrdU-only studies (Figures 1D and 2A), as might be predicted if AST-1 promotes the early release of BrdU-labeled cells from the immune system. According to our hypothesis, some of these newly released circulating cells migrate to and are incorporated into the niche, resulting in a "premature" peak of BrdU-labeled cells in the niche. We also conclude that peak F is composed of BrdU-labeled cells akin to those composing peak B (Figures 1D and 2A), but this may be delayed because the most mature cells in the APC and/or HPT were released prematurely and compose peak E, resulting in delayed release of additional cells from the source tissue.

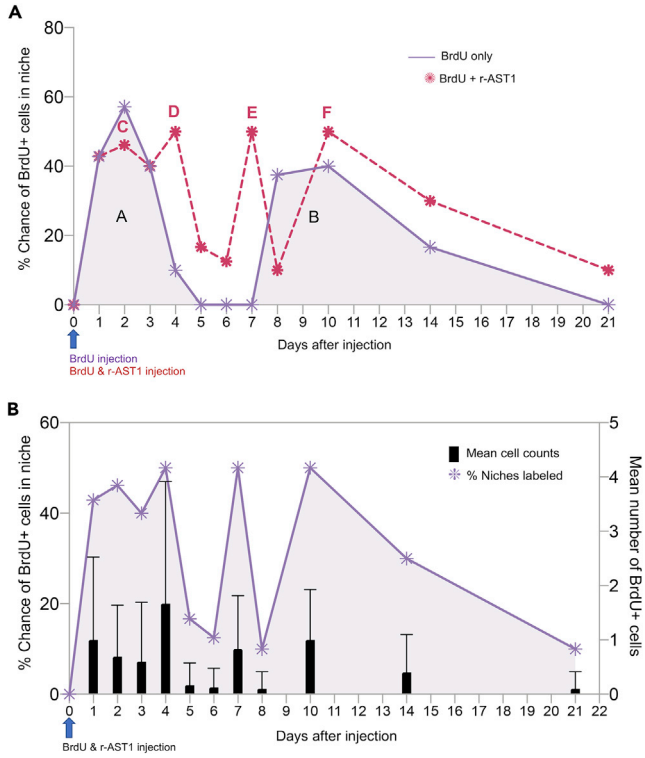

Figure 2. AST1 alters the timing of appearance of proliferating cells in the niche

(A) Comparison of the % chance of finding BrdU-labeled cells in the niche after a single BrdU injection on day 0 (purple, peaks A and B; graph adapted from Benton et al., 2014), and after simultaneous injection of BrdU plus r-AST1 on day 0 (red dashed graph, peaks C–F). For both experiments, animals were euthanized and brains dissected on days 1–8, 10, 14, and 21. Peaks in labeling are denoted by letters and are found on days 2 and 10 for the BrdU alone injection (Peaks A and B), and on days 2, 4, 7, and 10 for the BrdU plus r-AST1 injection (peaks C–F, indicated above each peak).

(B) The average number of BrdU-labeled cells in the niche (right *Y* axis) was calculated for each time point (bar graphs; mean ± SD) for the BrdU plus r-AST1 injection, and plotted with the % chance of finding a BrdU-labeled cell in the niche (left *Y* axis).

The average number of BrdU-labeled cells found in the niche at each time point is superimposed on the niche graph (Figure 2B, right *Y* axis). The numbers of cells at each sampling time roughly follows the pattern of the % chance of finding BrdU-labeled cells in the niche (left *Y* axis), rising and falling with the peaks, reinforcing the implications of these data.

Simultaneous injection of BrdU and r-AST1 therefore results in four distinct peaks in BrdU labeling (C–F) in the niche, compared with two peaks (cells intrinsic to the niche, followed by source-labeled cells) in earlier studies without r-AST1 (Benton et al., 2014). AST1 introduction also obliterates the gap period when no BrdU labeling was observed in previous studies, such that BrdU-labeled cells are observed in the niche at all time points. This is consistent with the hypothesis that AST1 treatment would advance the arrival of the late-appearing BrdU-labeled cells in the niche (i.e., peak B in the original studies without AST1; Benton et al., 2014), owing to the premature release of cells from the immune system.

AST-1 alters cell proliferation in the APC and HPT

As expected, r-AST1 injection also influences cell proliferation in the APC and HPT (Figures 3A–3C). On day 1, BrdU-labeled cells in the APC are reduced to fewer than 20% of all APC cells (red dashed line, Figure 3B), from >40% when only BrdU is injected (green line graph in 3B). The APC is completely depleted of BrdU labeled cells by day 4 following r-AST1 injection, whereas BrdU labeling is not fully depleted until day 8 in the BrdU-only injection experiment. These data indicate that r-AST1 injection results in a more rapid release of APC cells.

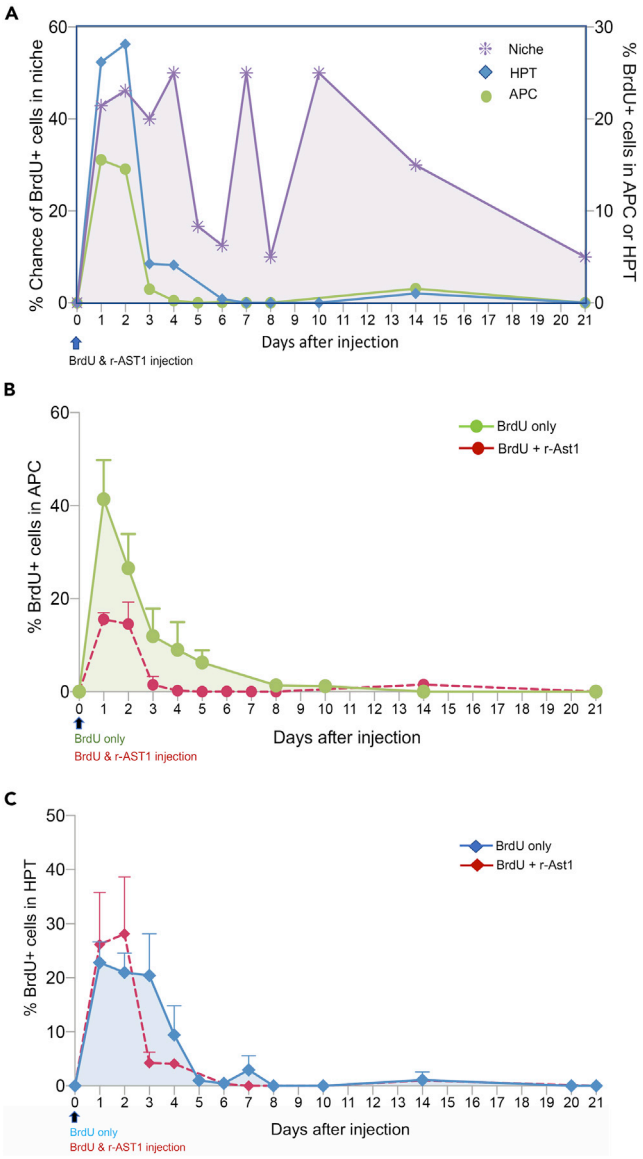

Figure 3. AST-1 alters cell release from the APC and HPT

After a simultaneous injection of BrdU and r-AST1 on day 0, brains, APC and HPT were dissected from groups of crayfish on days 1–8, 10, 14, and 21 post-injection. The % chance of finding BrdU-labeled cells in the niche, as well as the % of cells that were BrdU-labeled in the HPT and APC were determined for each time point. BrdU-labeled cells are found in the niche on all days, with peaks on days 2, 4, 7, and 10 (peaks C–F, Figure 2A)

(A) The dynamics of proliferation in the APC and HPT (right *Y* axis) are overlaid on the graph of BrdU-labeled cells in the niche (left *Y* axis) following a single injection of BrdU and r-AST1.

(B and C) The % BrdU-labeling in the APC (B) and HPT (C) is compared between experiments with BrdU-only (APC, green; HPT, blue) and BrdU plus r-AST1 (red dashed lines) injections. Error bars indicate standard deviations.

The influence of r-AST1 on the HPT is less striking, as the % BrdU labeling on day 1 after injection is similar to the BrdU-only study (Figures 3A and 3C). However, the decline in % BrdU labeling in the HPT is more rapid after r-AST1 injection (Figure 3C). Depletion of BrdU labeling in the HPT is similar with and without r-AST1 injection, occurring by day 5 or 6.

These studies demonstrate that altering the timeline of hemocyte release from the immune system with r-AST1 also changes the timing of appearance of BrdU-labeled cells in the niche, consistent with other data suggesting that the immune system replenishes the neural progenitors in the niche. Because AST1

has the greatest influence on the APC cell population (Figure 3B), causing the release of more than half of the BrdU-labeled cells by the first sampling point on day 1, we suggest that these cells contribute to the niche replenishment, although a contribution from the HPT cannot be ruled out, since AST1 accelerates the release of cells from both tissues – albeit more rapidly from the APC. According to this interpretation, the change in the behavior of APC cells may correlate with the appearance of peak E (Figure 2).

Hyaline cells proliferate *in vitro* and *in vivo* (Figure 4)

It has been reported that circulating hemocytes in crayfish proliferate rarely (Bauchau, 1981; Söderhäll et al., 2003; Li et al., 2021). We wanted to test this in *P. clarkii*, because this has important implications for these studies. Using a simple *in vitro* approach, the presence of BrdU labeling in hemocytes attached to lysine-coated glass coverslips was examined; hemocytes were withdrawn from crayfish 1 h prior to BrdU incubation, which lasted for 6 h.

All three classes of hemocytes were identified in these preparations: hyaline, semigranular, and granular (Figure 4A). Crustacean hemocytes are generally classified based on morphological criteria (Bauchau, 1981; Söderhäll, 2016), although details of form and function vary somewhat among species. In crayfish, the granular cells are the largest hemocytes, and are generally spherical or oval cells densely packed with granules; these are involved in phagocytosis and the proPO-activating system (Cerenius and Söderhäll, 2004, 2021). Semigranular cells are characterized by sparsely distributed small granules; these cells often have an elliptical shape and bipolar processes, and participate in encapsulation. The hyaline cells, the smallest of the three hemocyte types, contain large nuclei, minimal cytoplasm containing no or few granules, and their contributions to immune function are least well understood. These have been proposed to be immature or prematurely released prohemocytes (van de Braak et al., 2002; Lin and Söderhäll, 2011). Of these cell types, hyaline cells have the highest nuclear to cytoplasmic ratio, and granular cells have the lowest.

In our short-term *in vitro* experiments, nuclear BrdU labeling was evident only in the hyaline cells, which were quite numerous, in contrast to reports in other species (e.g., Li et al., 2021). Nuclear BrdU was found in 10–15% of hyaline cells that were identified, suggesting that this population is active in the cell cycle (Figures 4A–4C). Focal cytoplasmic labeling also was observed in granular cells (Figures 4B and 4D). Comparisons with published data and images (e.g., Yapici et al., 2015) indicate that the labeled regions may be individual lysosomes or endosomes. It is not known whether these cells may be actively involved in phagocytosis of BrdU-labeled cells, which would result in cytoplasmic labeling of the granular cell, or perhaps more likely, whether BrdU is passively taken up as the granular cells digest particles in the culture medium. Regardless of the underlying mechanism, a significant proportion of the granular cells contained this punctate cytoplasmic labeling.

In vivo studies of circulating hemocytes at various intervals after a single injection of BrdU into crayfish also suggest that hyaline cells are the only hemocytes that incorporate BrdU into the nucleus (Figures 4E–4H). Hemolymph samples taken at 6 h post-BrdU injection, the same BrdU exposure time used in the *in vitro* studies, are very similar to what was observed *in vitro*. That is, all three hemocyte types are present, hyaline cells are the most numerous cell type observed, and many of these have BrdU-labeled nuclei (Figures 4E and 4G). No other hemocyte labeling is observed. In hemolymph samples taken at 7 days post-BrdU injection (Figures 4F and 4H), the same interval used for adoptive transfers of hemocytes, hyaline cells continue to be the most numerous hemocyte type and nuclear labeling of these is frequently observed. However, cytoplasmic labeling of granular cells was not observed in these samples, as in the *in vitro* (Figures 4B and 4D) and adoptive transfer (Figures 5, 5D, 5E, 8A, and 8B) studies. Additional studies are underway to explore this difference among our preparations. Note that some circulating hemocytes illustrated in Figure 4 may not be fully mature forms, and therefore may not show all of the typical features of the mature cell types described above. Nevertheless, the identification of the BrdU-labeled hemocytes as hyaline cells is unequivocal.

These studies show that circulating hemocytes in *P. clarkii* do proliferate and that this is not a rare event. Second, hyaline cells appear to be the only variety of hemocyte that is active in the cell cycle, both *in vitro* and *in vivo*, at least under our experimental conditions.

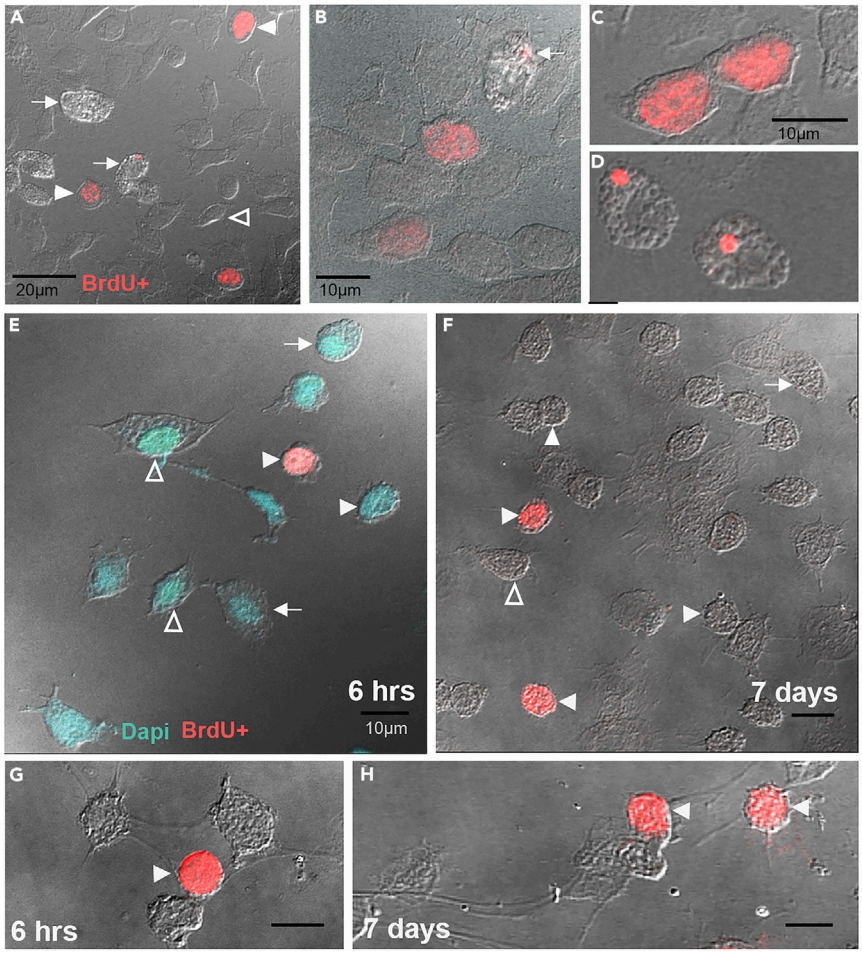

Figure 4. Hyaline cells proliferate *in vitro* (Figures 4A–4D) and *in vivo* (6-h samples: Figures 4E and 4G; 7-day samples: Figures 4F and 4H)

(A) Hemolymph was withdrawn from crayfish and hemocytes were attached to lysine-coated slides. All three hemocyte types can be identified in these samples: granular (arrows); semigranular (open arrowheads); hyaline (filled arrowheads). These hemocytes were treated with BrdU for 6 h, beginning 1 h after hemolymph was taken from the crayfish, and then processed immunocytochemically. Only hyaline cells in these samples contain labeled nuclei (BrdU, red), although not all hyaline cells are labeled. Many granular cells contain a small area of cytoplasmic labeling (arrow in the middle of the frame; see also B, D).

(B) Two hyaline cells containing nuclear BrdU labeling are shown, as well as one granular cell with an area of cytoplasmic labeling (arrow). Two unlabeled hyaline cells are also shown in the bottom right of this image.

(C and D) Higher magnification images are shown with (C) two hyaline cells containing nuclear labeling and (D) two granular cells with a small area of cytoplasmic labeling.

(E) *In vivo* 6 h post-BrdU injection. Hemolymph was withdrawn from crayfish that had been injected with BrdU 6 h earlier. Hemocytes were attached to lysine-coated slides, fixed and processed immunocytochemically. All three hemocyte types can be identified in these samples: granular (arrows); semigranular (open arrowheads); hyaline (filled arrowheads). Only hyaline cells in these samples contain labeled nuclei (BrdU, red), although not all hyaline cells are labeled.

(F) *In vivo* 7 days post-BrdU injection. Hemolymph was withdrawn from crayfish that had been injected with BrdU 7 days earlier, and hemocytes were attached to lysine-coated slides. All three hemocyte types could be identified in these samples, although only hyaline cell nuclei contain BrdU labeling. Examples of hyaline cells, two of which are labeled, and semigranular cells, which are not labeled, are illustrated.

(G) *In vivo* 6 h post-BrdU injection. Higher magnification, showing a BrdU-labeled hyaline cell (filled arrowhead) near unlabeled hemocytes.

(H) *In vivo* 7 days post-BrdU injection. Higher magnification, showing BrdU-labeled hyaline cells amidst unlabeled cells. Scale bars: (A) 20 μm; (B–H) 10 μm.

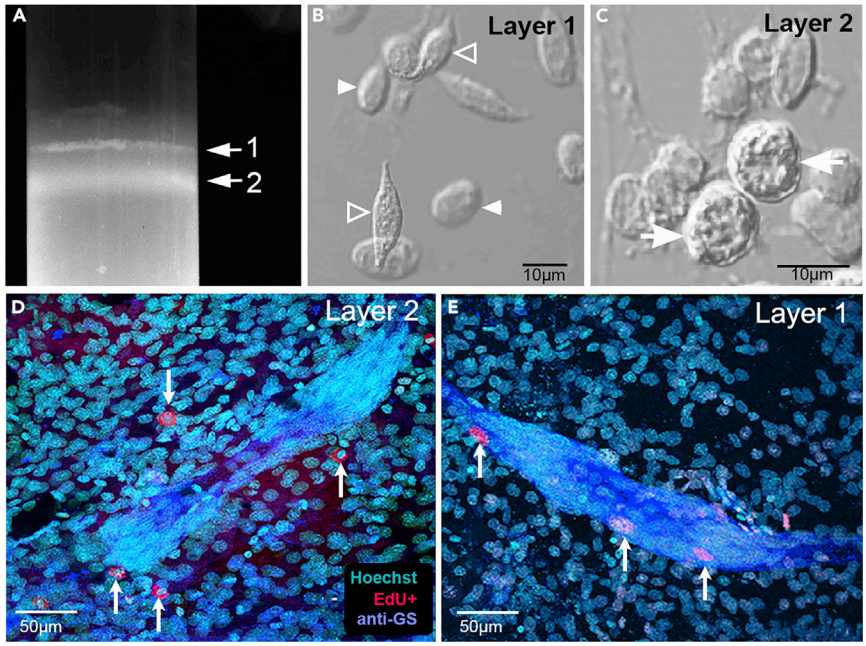

Figure 5. Hemocyte types are separated with Percoll gradients and adoptively transferred

(A) Hemolymph from donor crayfish containing EdU-labeled hemocytes was separated into two layers (1, 2) with Percoll gradients (see Methods for details).

(B) Layer 1 contains hyaline (filled arrowheads) and semigranular (open arrowheads) hemocytes. The hyaline cells have a narrow, clear rim of cytoplasm surrounding a large nucleus. Semigranular cells contain sparse granules and are often spindle-shaped in these preparations.

(C) Layer 2 contained granular hemocytes (arrows), which are spherical cells densely packed with granules.

(D) When hemocytes from layer 2 (granular cells, arrows) were injected into recipient crayfish, these were often found near, but never in, the niche of recipients. Characteristically, the EdU labeling observed was cytoplasmic, suggesting that EdU-labeled donor cells took up EdU during phagocytosis of debris, or perhaps by phagocytosis of other labeled hemocytes.

(E) When cells from layer 1 (hyaline and semigranular cells) were injected into recipient crayfish, cells with EdU nuclear labeling were observed in the niche (arrows) and were similar in size to the intrinsic niche cells. Scale bars: (B, C) 10 μm; (D, E) 50 μm.

Hemocyte types can be separated and adoptively transferred (Figures 5 and 6)

To further explore which hemocyte type is associated with adult neurogenesis, hemolymph was separated using Percoll Plus gradients, yielding viable cells that could then be used directly in adoptive transfers. However, the numbers of cells in each layer are reduced by the multiple cell transfers from the donor to gel to the recipient. Observation of hemocytes between these transfers also suggests that the number of viable cells decreases as the protocol progresses.

Separation of hemolymph from individual crayfish with Percoll Plus gradients resulted in two distinct bands (Figure 5A). Each of these was gently removed with a micropipette. Cell morphology in each band was then examined to determine whether the bands contained a relatively pure population of cells, and to identify the cell types. These studies demonstrated that layer 1 contains hyaline and semigranular hemocytes (Figure 5B). Layer 2, the deeper (heavier) band, contains granular cells (Figure 5C).

Adoptive transfers of specific hemocyte types

The goal of these studies was to ask whether a specific hemocyte class can be associated with the neurogenic lineage. Donor hemocytes were drawn on days 7–8 after EdU injection, around the time that source-labeled cells are beginning to appear in the niche following a single injection of a proliferation marker (Figure 1D), suggesting these are mature and competent to integrate into the niche (Benton et al., 2014). Following blood collection, hemolymph was separated into specific hemocyte types with Percoll gradients, and each layer from the gradient was transferred into different recipients, with one recipient receiving either layer 1or 2 cells from an individual donor crayfish.

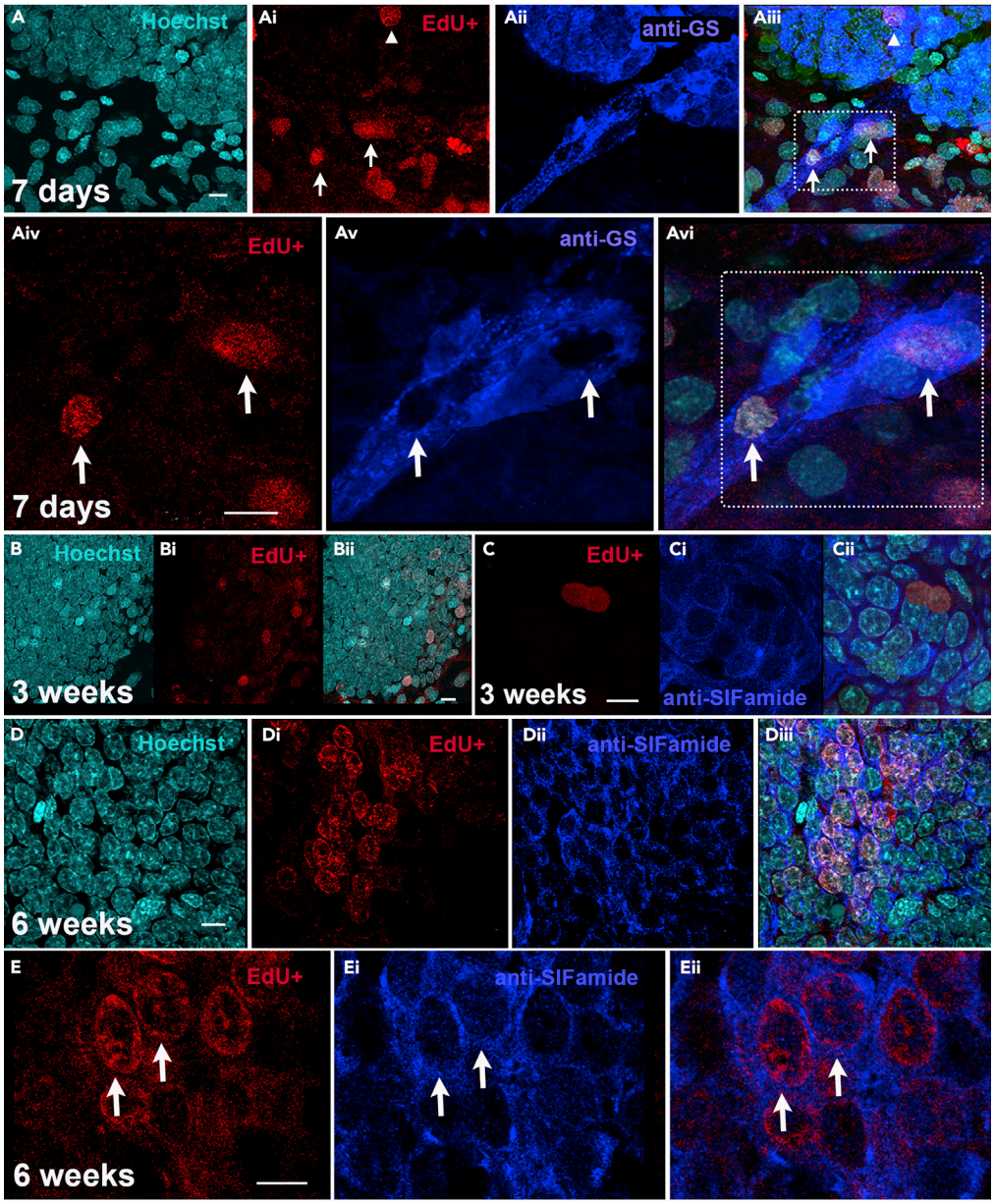

Figure 6. Adoptively transferred hemocytes from Percoll gradient layer 1 enter the neurogenic lineage

Hemolymph from donor crayfish containing EdU-labeled hemocytes was separated into two layers with Percoll gradients. Layer 1 cells (hyaline and semigranular hemocytes) were injected into recipient crayfish. Brains and associated niches are shown with EdU labeling that indicates the progression of donor hemocytes through the neurogenic lineage. Scale bars: 10 μm.

(A) EdU-labeled cells are observed in the streams (arrows) and proliferation zones (arrowhead) of Cluster 10 at 7 days after transfer of donor hemocytes from layer 1. A, Hoechst 33,342 (cyan); Ai, EdU cell labeling (red); Aii, anti-GS (blue). The GS antibody labeled all cells in the niche, streams and proliferation zones in *P. clarkii*. EdU-labeled cells are also observed in the vicinity that are not in the streams or cell cluster. The merged image (Aiii) illustrates the positions of these cells, as well as the location of the enlarged image shown in Aiv-Avi (dotted line box). These highly magnified images show the labeled cells (arrows) and their placement in the streams. The 'holes' in GS labeling (Av) are the positions of the EdU labeled cells (Aiv), shown merged in Avi.

(B and C) Three weeks after transfer of layer 1 cells from donor crayfish, single cells (B-Bii) and pairs of cells (C-Cii) are observed in Cluster 10. This pair of cells contains no SIFamide labeling (blue, Ci, Cii).

Figure 6. *Continued*
(D) Six weeks after transfer of layer 1 cells from donor crayfish, EdU-labeled cells are frequently found in clusters (Di), and cells in these clusters contain immunoreactivity for the neurotransmitter SIFamide (Dii, Diii). (E) In these higher magnification images taken six weeks after layer 1 transfer to a recipient crayfish, EdU-labeled cells are observed with anti-SIFamide labeling in the cytoplasm (arrows; Eii shows the merged image illustrating this feature).

After adoptive transfer of layer 2 (granular) cells (n = 12 brains, 21 niches), hemocytes with EdU-labeled nuclei are not observed in the niche, streams or cell clusters, although cells with cytoplasmic EdU labeling are found near the niche in these preparations (Figure 5D). In contrast, after adoptive transfers of layer 1containing hyaline and semigranular hemocytes (n = 14 brains, 24 niches), EdU-labeled cells (nuclear and/or cytoplasmic labeling) are observed in 29% of all niches in recipient crayfish; 8% contained cells with EdU nuclear labeling that overlaps completely with Hoechst labeling and without cytoplasmic EdU (Figure 5E). Cytoplasmically-labeled cells (see Figure 5D) likely result from phagocytic cells engulfing EdU-labeled cells, or alternatively, from passive uptake of EdU while ingesting cellular debris during the EdU labeling period in the donor. These were observed in samples of donor hemolymph (data not shown), in addition to *in vitro* hemocyte proliferation studies (Figures 4B and 4D), suggesting that at least some of these cells come from the donors in that condition.

Three days after transfer of layer 1 cells to recipients, EdU-labeled cells are found in the niches of recipient crayfish (Figure 5E). One week after the transfer, EdU-labeled cells are observed primarily in the streams and proliferation zones of cell Clusters 9 and 10 (Figure 6A). Three and six weeks after the transfer, EdU-labeled cells are frequently observed in Clusters 9 and 10. These cells have EdU-labeled nuclei and appear to have divided, as they tend to occur in pairs (Figures 6C and 6Cii) and groups (Figures 6D and 6E). Some of these cells contain immunoreactivity for the transmitter SIFamide (Figures 6Dii, 6Diii, 6Ei, and 6Eii), one of the transmitters normally expressed by many cells in Cluster 10 (Yasuda-Kamatani and Yasuda, 2006; Polanska et al., 2007) and others not (Figures 6Ci and 6Cii), possibly reflecting differences in their division and differentiation times.

Based on purely morphological criteria, results of prior *in vitro* studies have suggested that semigranular hemocytes are the most likely neural progenitor cell candidates (Benton et al., 2011). The present functional studies show that (1) incorporation into the niche is not observed after the transfer of EdU-labeled cells from layer 2 of Percoll Plus gradients containing granular cells (Figures 5C and 5D). (2) Labeled cells from layer 1of these gradients (containing hyaline and semigranular hemocytes) readily integrate into the niche, and are later found in the migratory streams and brain clusters. (3) Many labeled cells in Clusters 9 and 10 that result from layer 1cell transfers express transmitter, suggesting that adoptively transferred EdU-labeled hemocytes can generate cells with neural properties. Taken together with the finding that hyaline cells are the only hemocyte type that incorporates proliferation markers, these adoptive transfer findings indicate that hyaline cells are the prime neural progenitor cell candidates.

Adoptive transfers of APC and HPT cells have also been attempted, with the hope that the specific tissue source of the hemocytes might be identified. However, these cells never integrated among the niche cells as hemocytes do, although they occasionally were found loosely attached to the edge of a niche. These results are reminiscent of our findings with HPT cells *in vitro*, which also were not attracted to the niche in a previous study (Benton et al., 2011). Our assumption at that time was that cells extracted from the HPT would be immature and therefore not competent to be attracted to the niche. This hypothesis continues to be the most attractive interpretation of our findings with adoptive transfers of APC and HPT cells.

Serotonin regulates THC and alters adoptive transfer outcomes (Figures 7 and 8)

In the crayfish *P. leniusculus*, 5-HT regulates the expression of the cytokine AST1, which, in turn, regulates hematopoiesis (Lin et al., 2010; Lin and Söderhäll, 2011; Noonin, 2018). Consistent with those findings, r-AST1 injection results in higher THC in *P. clarkii* and also increases proliferation of cells in the niche-stream lineage that leads to the production of adult-born neurons (Benton et al., 2014). In addition, 5-HT (10^{-9} M) increases the number of cells in the neurogenic niche without increasing the incorporation rate of proliferation markers, suggesting that there must be an influx of cells to the niche (Benton et al., 2011). Finally, we have demonstrated here that by increasing AST1 levels, the timing of appearance of labeled neural progenitors in the niche can be manipulated. Taken together, these data indicate

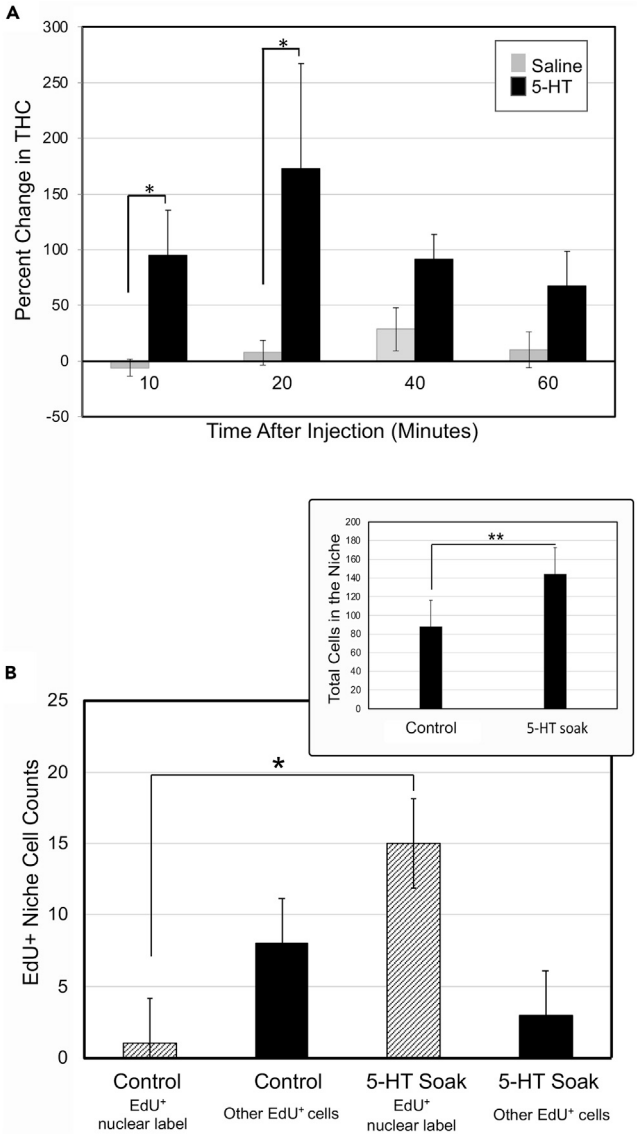

Figure 7. 5-HT regulates THC and alters adoptive transfer outcomes

(A) Injection of 5-HT into crayfish leads to maximal THC increases by 20 min post-injection. Twenty microliters of hemolymph was collected from crayfish prior to experimentation in order to determine a pre-injection THC. After allowing crayfish to rest for 24 h, they were injected with saline or 5-HT and bled again at a specified time point (*x* axis) following the injection to determine a post-injection THC. The % change was determined as: (post-injection THC – pre-injection THC/pre-injection THC) * 100. Grey bars represent the average percent change in THC of animals injected with saline, and black bars represent average % change in THC of animals injected with 5-HT. Comparisons between groups were made with one-way ANOVA analysis followed by Tukey's multiple comparison tests. Error bars indicate the standard error of the mean (SEM). Asterisks indicate significant difference from saline control (independent samples *t*-test, 10 min, $p = 0.018$; 20 min, $p = 0.021$). For the 5-HT group (black bars), for the four time points (10, 20, 40, and 60 min), sample size $n = 11$, 9, 10, and 8 animals, respectively. For the saline group (grey bars), $n = 8$, 9, 9, and 8, respectively.

(B,Inset) Recipient crayfish were soaked in 5-HT for 24 h after adoptive transfer of hemocytes from donor crayfish. The total number of niche cells increases, despite the potential immune response to the introduction of foreign cells. This effect of 5-HT has also been observed without adoptively transferred cells (Benton et al., 2011). The niches of 5-HT-treated crayfish increase by an average of 65.5% cells, which represents a significant increase compared with the control crayfish maintained in pond water (independent samples *t*-test, $p = 0.001$). Error bars indicate SEM; $n = 11$ niches per group.

(B) After the adoptive transfer of EdU-labeled donor hemocytes, recipient crayfish were soaked in pond water alone (control) or pond water + 5-HT (10^{-9} M) (5-HT soak). 40% (control) and 50% (5-HT-soaked) of niches contained EdU-labeled cells; therefore, the number of recipient niches is not substantially altered by increased levels of 5-HT. However,

Figure 7. *Continued*
the numbers of donor hemocytes that are incorporated into niches increases after 5-HT incubation of recipients, and the types of labeled cells observed are also altered. In 5-HT-treated recipients, 83% of labeled niche cells (15) contained EdU nuclear labeling and were elliptical with no (or sparse) granules; these are similar in size and shape to resident niche cells. In pond water controls, only one cell contained nuclear label (bars with diagonal lines) and had these morphological features. 5-HT treatment of recipients tends to have the opposite influence on "other EdU-labeled cells" (cytoplasmic labeling with or without nuclear labeling). 5-HT treatment resulted in a reduction in the mean numbers of these "other EdU+" cells (black bars). *t*-tests comparing the data for each of these labeling types revealed a significant difference in "EdU nuclear label" ($p = 0.017$) between the 5-HT soak and control groups, but no statistical difference in the "other EdU + cells" ($p = 0.68$). Error bars represent SEM; $n = 12$ niches per group.

overlapping roles for 5-HT and AST1 in adult neurogenesis, reinforcing the proposal that these two molecules may serve as communication links between the nervous system and immune system (Beltz and Benton, 2017).

Increased 5-HT results in higher total hemocyte counts (THC)

We sought to determine if 5-HT influences THC in *P. clarkii*, as in *P. leniusculus* (Noonin, 2018). Small hemolymph samples (30–40 μL) were collected from crayfish ($n = 72$) 24 h prior to any experimental manipulation to obtain a baseline THC. Either crayfish saline or serotonin creatinine sulfate in saline was then injected into the thoracic cavity of crayfish, to raise 5-HT levels to ~5 nM (see Methods). Post-injection THCs were then determined at intervals (10, 20, 40, and 60 min) after 5-HT injection. The % change in hemolymph counts relative to baseline for each group of crayfish was then determined (Figure 7A). A one-way ANOVA followed by Tukey's HSD demonstrated that crayfish injected with 5-HT exhibited significant increases in THC relative to saline controls. The largest increase in THC observed was 20 min after 5-HT injection. Independent samples *t*-tests revealed that the average % change in THCs 10 and 20 min post-injection was significantly higher than saline controls ($p = 0.018$ and 0.021, respectively). The increase in THC in response to 5-HT was anticipated, since 5-HT increases the AST1 expression (Beltz and Benton, 2017; Noonin, 2018). However, the very rapid response in THC and the fact that the timing of the hemocyte response to 5-HT appears to be concentration-dependent (data not shown), suggest that there may be a direct influence of 5-HT on hemocyte release, in addition to the AST1-mediated discharge of cells (Figures 3B and 3C; Noonin, 2018; Fukumura, 2019).

5-HT increases the total number of niche cells in recipient crayfish after adoptive transfer Previous studies have shown that in crayfish incubated in artificial pond water with added 5-HT, the neurogenic niches visibly swell and contain increased numbers of cells (Benton et al., 2011). When crayfish that received labeled donor blood cells were soaked in pond water and 5-HT for 24 h after the hemolymph transfer, the number of cells in their niches ($n = 11$) increased by 67% compared with niches of hemolymph recipients that were maintained in pond water alone ($n = 11$) (Figure 7B, inset). This difference is statistically significant (*t*-test, $p = 0.001$) and demonstrates that despite any immune response that may be triggered by the blood cell transfer, 5-HT increases niche size and cell numbers, as it does in crayfish that have not received adoptively transferred cells.

5-HT increases hemocyte incorporation into the niche

Adoptive transfers of EdU-labeled hemolymph from donor crayfish have been used to test whether hemocytes can serve as neural progenitors (Benton et al., 2014), and to test which hemocyte type is involved (Figures 5 and 6). However, quantitative studies have shown that the incorporation rate of donor hemocytes can be very low (Brenneis and Beltz, 2020).

In the current experiments, the recipients of EdU-labeled donor hemolymph were treated with 5-HT, to ask whether the outcomes of the adoptive transfers are altered. Whereas the proportions of recipient niches containing labeled cells are similar in controls and 5-HT-treated groups, the numbers and *types* of labeled cells incorporated into the niches are altered (Figure 7B). In hemocyte recipients maintained in pond water, ~40% of the niches (5 of 12 niches) contained a total of nine EdU-labeled cells; eight of which contained cytoplasmic labeling. Only one niche contained a cell with nuclear labeling (11% of labeled cells) (Figure 7B). This low yield is reminiscent of adoptive transfer data published previously (Brenneis and Beltz, 2020). A very different situation was observed in the 5-HT-treated recipients. In total, 50% (6 of 12 niches) of niches contained a total of 18 EdU-labeled cells. Of these, 83% (15 cells) contained exclusively EdU nuclear labeling; three cells had cytoplasmic labeling (Figure 7B).

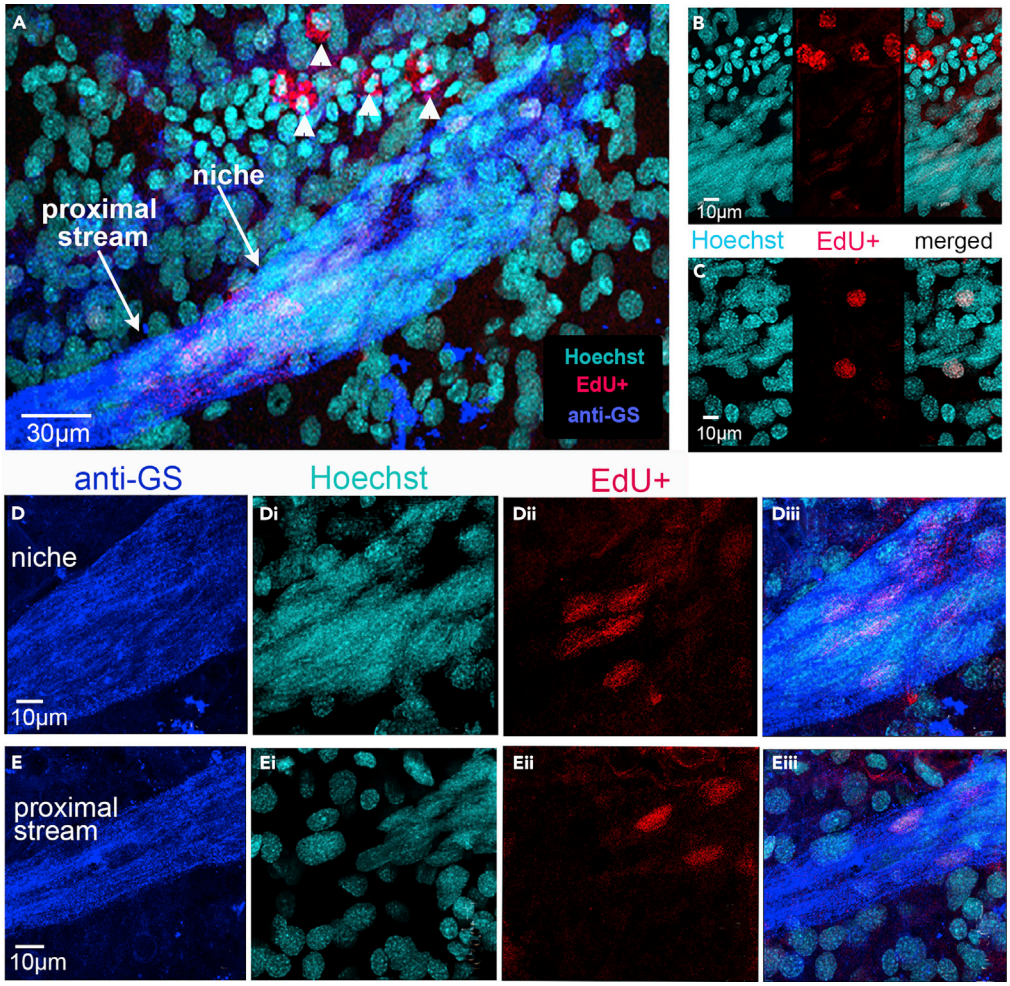

Figure 8. 5-HT increases hemocyte incorporation into the niche

(A) After 5-HT treatment of recipient crayfish following adoptive transfer of EdU-labeled hemocytes from donor crayfish, cells containing EdU nuclear labeling (red) are found in the niche (A, Dii, Diii) and proximal stream (A, Eii, Eiii) in recipient crayfish. Cells containing cytoplasmic EdU labeling are also seen in the vicinity of the niche in A (arrowheads above niche). (B and C) Additional EdU-labeled cells are observed near but not in the niche, some with cytoplasmic EdU (B) and others with nuclear EdU (C); Hoechst and EdU channels are shown separately, with the merged channel on the right. The cell labeling in the niche (D) is illustrated with images of individual fluorescence channels (D, anti-GS; Di, Hoechst; Dii, EdU) and the merged image (Diii). EdU-labeled cells are also observed in the proximal regions of the streams in separate and merged images (A, Eii, Eiii). Scale bars: (A) 30 μm; (B–E) 10 μm.

The major difference between these groups, therefore, is that the 5HT-treated crayfish had many more EdU nuclear-labeled cells in the niche than those in the control group (83 vs. 11% of total labeled cells; *t*-test, $p < 0.02$) (Figure 7B). The number of niches that are receptive to transferred cells is not dramatically altered by 5-HT, but 5-HT *does influence* the numbers and types of cells that the receptive niches accept, biasing the niche toward the incorporation of cells containing nuclear labeling with EdU (Figures 7 and 8). These cells can be visualized in the niche (Figures 8A, 8Dii, and 8Diii) and proximal streams (Figures 8A, 8Eii, and 8Eiii). In contrast, cells with cytoplasmic EdU labeling are observed near, but not inside, the niche (Figures 8A and 8B). These experiments therefore show that the incorporation of hemocytes into the niche is regulated by 5-HT. This finding further implies that the incorporation of hemocytes into the niche may be controlled by many hormonal agents circulating in the hemolymph, either through their regulation of hemocyte type or THC (see e.g., Tong et al., 2020), or by acting on the niche itself.

Conclusions

Several important conclusions can be drawn from these experiments. First, the dynamics of proliferation and release of APC and HPT cells into the circulation are distinct, although these two tissues are in closeness, proximity and both function as part of the immune system. Whereas the data presented here allow only for correlations between the appearance of labeled cells in the niche (Figure 1D) and the proliferation dynamics in the hematopoietic tissues, these results also provide a foundation for comparing the influence of AST1, which is known to promote the differentiation and release of hemocytes from the immune system. We hypothesized that an increase in AST1 would advance the appearance of the delayed peak "B" of the BrdU-only experiment (Figure 1D). Indeed, r-AST1 injection results in the appearance of BrdU-labeled cells in the niche during the "gap" period identified in BrdU-only studies (Figure 1D); thus, labeled cells are found in the niche throughout the entire sampling period (Figure 2B). These results demonstrate that altering the release of hemocytes from the immune system also alters the timing of appearance of labeled cells in the niche, further supporting the proposal that the immune system is responsible for replenishing the neural progenitor population in the niche. These findings therefore indicate that the specific timing of hemocyte incorporation into the niche is highly modifiable and prone to physiological and environmental influences that alter AST1 levels.

Percoll gradients allowed the separation of the three hemocyte types into two distinct bands: Layer one contains hyaline and semigranular cells, and layer 2 contains granular cells. The adoptive transfers of each of the Percoll layers to recipient crayfish indicate that cells from layer 1, but not layer 2, are readily incorporated into recipient niches. This finding suggests that semigranular or hyaline cells (Figure 5B) are the most likely neural progenitor candidates. In previous studies, we proposed based solely on purely morphological criteria that semigranular cells are the presumptive neural progenitors (Benton et al., 2011). However, the present functional studies show that hyaline cells are the only hemocytes that are actively in the cell cycle and therefore able to incorporate proliferation markers. This knowledge, combined with the successful adoptive transfers of EdU-labeled Percoll layer 1 hemocyte types (hyaline and semigranular), allows us to propose with confidence that hyaline cells are the prime neural progenitor cell candidates. Whether hyaline cells are multipotent stem cells or serve only as neural progenitors remains to be tested.

Serotonergic modulation of hemocyte incorporation into recipient niches following adoptive transfers from donor crayfish indicates a central role for this monoamine in coordinating the immune and neural responses. These findings further suggest that the replenishment of niche cells by hemocytes will vary as the hormonal status of the crayfish fluctuates, dependent on seasonality, circadian variations, stress, and other factors that influence 5-HT levels and the proportion and numbers of the three types of hemocytes. Ultimately, the fact that hemocyte incorporation into the niche can be regulated by physiologically relevant concentrations of 5-HT, and that AST1 levels modulate the timing of hemocyte release and incorporation into the niche, provide strong evidence in favor of our hypothesis that the immune system plays a pivotal role in supplying neural progenitors underlying adult neurogenesis in crayfish.

Limitations of the study

The current study demonstrates that the immune and nervous systems contribute in critical ways to adult neurogenesis in an invertebrate model, the crayfish. Limitations include a lack of quantitative information about the three hemocyte types under control conditions, and in relation to the actions of serotonin and AST1. The blood cell lineage in crayfish also is highly debated, and a clearer appreciation of the cellular relationships leading to the production of hyaline, semigranular, and granular cells would inform their roles in adult neurogenesis. Finally, whether the neural progenitor cells – which we propose are hyaline cells – are pluripotent or have a restricted fate in the production of neurons, is critical knowledge needed to more fully understand this system.

STAR★METHODS

Detailed methods are provided in the online version of this paper and include the following:

- KEY RESOURCES TABLE
- RESOURCE AVAILABILITY
  - Lead contact
  - Materials availability
  - Data and code availability

ACKNOWLEDGMENTS

The authors thank Pat Carey, Valerie LePage, and Nancy Thompson of the Wellesley College Animal Facility for the care of crayfish used in these experiments. This project was supported by National Science Foundation grants to BSB (NSF-IOS-1456918 and 1656103).

AUTHOR CONTRIBUTIONS

Project administration, validation, and funding acquisition, B.S.B.; conceptualization, B.S.B., J.L.B.; writing original manuscript draft, B.S.B., J.L.B.; project supervision and mentorship, J.L.B., P.G.C.S., B.S.B.; experiments and data analysis, J.L.B., J.L., E.W., Y.F., V.C.Q., P.G.C.S., A.J.E.; review and editing of the manuscript and visualization of data, all authors.

DECLARATION OF INTERESTS

The authors declare no competing interests.

INCLUSION AND DIVERSITY

We worked to ensure sex balance in the selection of non-human subjects. One or more of the authors of this paper self-identifies as an underrepresented ethnic minority in science. While citing references scientifically relevant for this work, we also actively worked to promote gender balance in our reference list.

Received: September 20, 2021
Revised: December 12, 2021
Accepted: February 24, 2022
Published: April 15, 2022

REFERENCES

Bauchau, A.G. (1981). Crustaceans. In Invertebrate Blood Cells, *Vol 2*, N.A. Ratcliffe and A.F. Rowley, eds. (Academic Press), pp. 385–420.

Beltz, B., and Benton, J. (2017). From blood to brain: adult-born neurons in the crayfish brain are the progeny of cells generated by the immune system. Front. Neurosci. *11*, 662. https://doi.org/10.3389/fnins.2017.00662.

Benton, J.L., Zhang, Y., Kirkhart, C.R., Sandeman, D.C., and Beltz, B.S. (2011). Primary neuronal precursors in adult crayfish brain: replenishment from a non-neuronal source. BMC Neurosci. *12*, 53. https://doi.org/10.1186/1471-2202-12-53.

Benton, J.L., Chaves da Silva, P.G., Sandeman, D.C., and Beltz, B.S. (2013). First-generation neuronal precursors in the crayfish brain are not self-renewing. Int. J. Dev. Neurosci. *31*, 657–666. https://doi.org/10.1016/j.ijdevneu.2012.11.010.

Benton, J.L., Kery, R., Li, J., Noonin, C., Söderhäll, I., and Beltz, B.S. (2014). Cells from the innate immune system generate adult-born neurons in crayfish. Dev. Cell *30*, 322–333. https://doi.org/10.1016/j.devcel.2014.06.016.

Brenneis, G., and Beltz, B.S. (2020). Adult neurogenesis in crayfish: origin, expansion, and migration of neural progenitor lineages in a pseudostratified neuroepithelium. J. Comp. Neurol. *528*, 1459–1485. https://doi.org/10.1002/cne.24820.

Cerenius, L., and Söderhäll, K. (2004). The prophenoloxidase-activating system in invertebrates. Immunol. Rev. *198L*, 116–126. https://doi.org/10.1111/j.0105-2896.2004.00116.x.

Cerenius, L., and Söderhäll, K. (2021). Immune properties of invertebrate phenoloxidases. Dev. Comp. Immunol. *122*, 104098. https://doi.org/10.1016/j.dci.2021.104098.

Chaves da Silva, P.G., Benton, J.L., Sandeman, D.C., and Beltz, B.S. (2013). Adult neurogenesis in the crayfish brain: the hematopoietic anterior proliferation center has direct access to the brain and stem cell niche. Stem Cell Dev *22*, 1027–1041. https://doi.org/10.1089/scd.2012.0583.

Chucholl, C. (2011). Population ecology of an alien "warm water" crayfish (*Procambarus clarkii*) in a new cold habitat. Knowl. Managt. Aquat. Ecosyst. *401*, 29. https://doi.org/10.1051/kmae/2011053.

Fukumura, Y. (2019). The Serotonin Hypothesis of Adult Neurogenesis (Wellesley College Honors Thesis).

Kim, Y.F., Sandeman, D.C., Benton, J.L., and Beltz, B.S. (2014). Birth, survival and differentiation of neurons in an adult crustacean brain. Dev. Neurobiol. *74*, 602–615. https://doi.org/10.1002/dneu.22156.

Li, F., Zheng, Z., Li, H., Fu, R., Xu, L., and Yang, F. (2021). Crayfish hemocytes develop along the granular cell lineage. Sci. Rep. *11*, 13099. https://doi.org/10.1038/s41598-021-92473-9.

Lin, X., and Söderhäll, I. (2011). Crustacean hematopoiesis and the astakine cytokines. Blood *117*, 6417–6424. https://doi.org/10.1182/blood-2010-11-320614.

Lin, X., Novotny, M., Söderhäll, K., and Söderhäll, I. (2010). Ancient cytokines, the role of astakines as hematopoietic growth factors. J. Biol. Chem. *285*, 28577–28586. https://doi.org/10.1074/jbc.M110.138560.

Noonin, C. (2018). Involvement of serotonin in crayfish hematopoiesis. Dev. Comp. Immunol. *86*, 189–195. https://doi.org/10.1016/j.dci.2018.05.006.

Noonin, C., Lin, X., Jiravanichpaisal, P., Söderhäll, K., and Söderhäll, I. (2012). Invertebrate hematopoiesis: an anterior proliferation center as a link between the hematopoietic tissue and the brain. Stem Cell Dev *21*, 3173–3186. https://doi.org/10.1089/scd.2012.0077.

Polanska, M.A., Yasuda, A., and Harzsch, S. (2007). Immunolocalization of crustacean-SIFamide in the median brain and eyestalk neuropils of the marbled crayfish. Cell Tiss. Res. *330*, 331–344. https://doi.org/10.1007/s00441-007-0473-8.

Rhodes, C.P. (1982). The relationship between size and blood volume in the crayfish *Austropotamobious pallipes* (Lereboullet) (Decapoda, Astacidea). Crustaceana *43*, 51–59.

Scalici, M., Cheisa, S., Scuderi, S., Celauro, D., and Gibertini, G. (2010). Population structure and dynamics of *Procambarus clarkii* (Girard, 1852) in a Mediterranean brackish wetland (Central Italy). Biol. Invasions *12*, 1415–1425. https://doi.org/10.1007/s10530-009-9557-6.

Söderhäll, I. (2016). Crustacean hematopoiesis. Dev. Comp. Immunol. *58*, 129–141. https://doi.org/10.1016/j.dci.2015.12.009.

Söderhäll, I., Bangyeekhun, E., Mayo, S., and Söderhäll, K. (2003). Hemocyte production and maturation in an invertebrate animal; proliferation and gene expression in hematopoietic stem cells of *Pacifastacus leniusculus*. Dev. Comp. Immunol. *27*, 661–672. https://doi.org/10.1016/S0145- 305X(03)00039-9.

Söderhäll, I., Kim, Y.A., Jiravanichpaisal, P., Lee, S.Y., and Söderhäll, K. (2005). An ancient role for a prokineticin domain in invertebrate hematopoiesis. J. Immunol. *174*, 6152–6160. https://doi.org/10.4049/jimmunol.174.10.6153.

Söderhäll, K., and Smith, V.J. (1983). Separation of the haemocyte populations of *Carcinus maenas* and other marine decapods, and prophenoloxidase distribution. Dev. Comp. Immunol. *7*, 229–239. https://doi.org/10.1016/0145-305x(83)90004-6.

Song, C.K., Johnstone, L.M., Edwards, D.H., Derby, C.D., and Schmidt, M. (2009). Cellular basis of neurogenesis in the brain of crayfish, Procambarus clarkii: neurogenic complex in the olfactory midbrain from hatchlings to adults. Arthropod Struct. Dev. *38*, 339–360. https://doi.org/10.1016/j.asd.2008.12.004.

Sullivan, J.M., and Beltz, B.S. (2005). Newborn cells in the adult crayfish brain differentiate into distinct neuronal types. J.Neurobiol. *65*, 157–170. https://doi.org/10.1002/neu.20195.

Sullivan, J.M., Benton, J.L., Sandeman, D.C., and Beltz, B.S. (2007). Adult neurogenesis: a common strategy across diverse species. J. Comp. Neurol. *500*, 574–584. https://doi.org/10.1002/cne.21187.

Tong, R., Pan, S., Pan, L., and Zhang, L. (2020). Effects of biogenic amines on the immune response and immunoregulation mechanism in hemocytes of *Litopenaeus vannamei* in vitro. Mol. Immunol. *128*, 1–9. https://doi.org/10.1016/j.molimm.2020.09.021.

van de Braak, C.B.T., Botterblom, M.H.A., Liu, W., Taverne, N., van der Knaap, W.P.W., and Rombout, J.H.W.M. (2002). The role of the haematopoietic tissue in haemocyte production and maturation in the black tiger shrimp (*Penaeus monodon*). Fish Shellfish Immunol. *12*, 253–272. https://doi.org/10.1006/fsim.2001.0369.

Yapici, N., Bi, Y., Li, P., Chen, X., Yan, X., Mandalapu, S.R., Faucett, M., Jockusch, S., Ju, J., Gibson, K.M., et al. (2015). Highly stable and sensitive fluorescent probes (LysoProbes) for lysosomal labeling and tracking. Sci. Rep. *5*, 8576. https://doi.org/10.1038/srep08576.

Yasuda, A., Yasuda-Kamatani, Y., Nozaki, M., and Nakajima, T. (2004). Identification of GYRKPPFNGSIFamide (crustacean-SIFamide) in the crayfish *Procambarus clarkii* by topological mass spectrometry analysis. Gen. Comp. Endrocrinol. *135*, 391–400. https://doi.org/10.1016/j.ygcen.2003.10.001.

Yasuda-Kamatani, Y., and Yasuda, A. (2006). Characteristic expression patterns of allatostatin-like peptide, FMRFamide-related peptide, orcokinin, tachykinin-related peptide, and SIFamide in the olfactory system of crayfish *Procambarus clarkii*. J. Comp. Neurol. *496*, 135–147. https://doi.org/10.1002/cne.20903.

Zhang, Y., Allodi, S., Sandeman, D.C., and Beltz, B.S. (2009). Adult neurogenesis in the crayfish brain: proliferation, migration and possible origin of precursor cells. Dev. Neurobiol. *69*, 415–436. https://doi.org/10.1002/dneu.20717.

STAR★METHODS

KEY RESOURCES TABLE

REAGENT or RESOURCE	SOURCE	IDENTIFIER
Antibodies		
Mouse anti-BrdU-Alexa Fluor® 488 (BrdU Monoclonal Antibody MoBU-1, Alexa Fluor 488)	ThermoFisher Scientific (Invitrogen)	Cat #B35130; RRID: AB_2536434
Mouse anti-glutamine synthetase (GS)	BD Biosciences	Cat #610517; RRID: AB_2313837
Rat anti-BrdU-Alexa Fluor® 555	Abcam	Cat #ab221240; RRID: AB_2893129.
Rabbit anti-SIFamide	Gift from Dr. A. Yasuda (Suntory Institute for Bioorganic Research, Osaka Japan) Yasuda et al., 2004; Yasuda-Kamatani and Yasuda, 2006; Polanska et al., 2007	N/A
AffiniPure goat anti-rabbit IgG (H+L) (minus x human, mouse, rat serum proteins) conjugated to Cy5	Jackson ImmunoResearch Laboratories	Cat #111-175-144; RRID: AB_2338013
Goat anti-mouse IgG DyLight 649	Jackson ImmunoResearch Labs	Cat#205-492-176; RRID: AB_2339069
Chemicals, peptides, and recombinant proteins		
5-bromo-2′-deoxyuridine (BrdU)	Millipore Sigma	Cat #19-160
4% paraformaldehyde	Fisher Scientific (EM Sciences)	Cat #50-259-99
Triton X-100	Sigma-Aldrich	Cat #X100
Propidium iodide	ThermoFisher (Invitrogen™)	Cat #P3566
Hoechst 33342	ThermoFisher Scientific	Cat #H3570
DAPI	ThermoFisher Scientific	Cat #62248
Trypan blue, 4% solution	ThermoFisher Scientific	Cat #15250061
Serotonin creatinine sulfate	Millipore Sigma	Cat #H7752
Fluoro-Gel	EM Sciences	Cat #17985-10
Recombinant-astakine 1 protein (r-AST1)	Gift from Irene Söderhäll (Uppsala University, Sweden). Method in Lin et al., 2010	N/A
Percoll Plus	GE Healthcare Life Sciences (now Cytiva)	Cat #17544501
Critical commercial assays		
CLICK-iT™ EdU Cell Proliferation Kit for Imaging, Alexa Fluor™ 488 dye	ThermoFisher Scientific (Invitrogen)	Cat #C10337
Experimental models: Organisms/strains		
Procambarus clarkii (red swamp crayfish)	Atchafalaya Biological Supply Co	N/A
Procambarus clarkii (red swamp crayfish)	Carolina Biological Supply Co.	N/A
Software and algorithms		
JMP Data Analysis Software	SAS Institute	https://www.jmp.com/en_us/software/data-analysis-software.html
IBM SPSS Statistics	IBM Corp	https://www.ibm.com/analytics/spss-statistics-software RRID: SCR_019096

RESOURCE AVAILABILITY

Lead contact

Further information and requests for resources and reagents should be directed to and will be fulfilled by the lead contact, Barbara Beltz (bbeltz@wellesley.edu).

Materials availability

This study did not generate new unique reagents.

Data and code availability

- No original code was generated in this study.
- No standardized datatypes were generated in this study, and therefore have not been deposited in a public repository.
- All data and analytical methods reported in this paper will be shared by the lead contact upon request.
- Any additional information required to reanalyze the data reported in this paper is available from the lead contact on request.

EXPERIMENTAL MODEL AND SUBJECT DETAILS

Adult freshwater crayfish (*Procambarus clarkii*) were obtained from Atchafalaya Biological Supply Co. (Raceland, LA 70394) and Carolina Biological Supply Co (Burlington, NC), and were maintained in the Animal Care Facility at Wellesley College. Crayfish were kept at room temperature in a 12:12 light:dark cycle in aquaria containing aerated artificial pond water (double-distilled water with added trace minerals and buffered using sodium bicarbonate) as well as artificial plants, PVC tubing and ceramic mugs for shelter and habitat enrichment. Both male and female crayfish were used in all experiments, although these were not scored independently; egg-bearing females were removed from the cohort. Previous work in *P. clarkii* has found no sex-related differences in the parameters of adult neurogenesis examined in the present study. Carapace length (CL;to the nearest millimeter) was measured as the length of the animal from the back of the eye socket to the posterior margin of the thoracic cavity.

METHOD DETAILS

Cell proliferation studies (APC and HPT) (Figure 1)

BrdU labeling and quantification of APC and HPT cells

BrdU (Millipore Sigma) (20 μL/gm of body weight of 5 mg/mL saline; saline: 205mM NaCl, 5.4mM KCl, 34.4 mM $CaCl_2$, 1.2 mM $MgCl_2$, and 2.4 mM NaHCO3) was injected into the ventral hemolymph sinus of crayfish (30-35 mm CL). All injections were done in the morning (09:00-11:00) of Day 0. At intervals between days 1 and 21 following BrdU injection, groups of crayfish were sacrificed and APC and HPT samples were dissected and fixed overnight at 4°C in 4% paraformaldehyde in 0.1 M phosphate buffer (PB; 20 mM NaH_2PO_4, 80 mM Na_2HPO_4; pH 7.4). Tissues were removed from fixative, rinsed for 1.5 hours in 0.3% Triton X-100 in 0.1 M phosphate buffer (PBTx), soaked in 2N HCl for 30 minutes, and rinsed again in PBTx for 1.5 hours. APC and HPT were incubated overnight at 4 °C in mouse anti-BrdU antibody conjugated to Alexa Fluor® 488 (1:20 in PBTx) (ThermoFisher, B351309). All tissues were then rinsed in PBTx for 1.5 hours. Tissues were treated with the nucleic acid stain propidium iodide (PI; 0.5 μM in PBTx; ThermoFisher, P3566), rinsed several times in PB, and mounted in Fluoro-Gel (Electron Microscopy Sciences, 17985-10). Slides were allowed to set for two days at room temperature prior to storage at 4°C.

All tissue preparations were analyzed using a Leica TCS SP5 confocal microscope. Four images were taken on each side of the APC (see regions circled in purple in Figure 1A), and two images were taken bilaterally in the posterior region on each side of the HPT, adjacent to the dorsal artery (regions circled in red in Figure 1A). These regions were chosen due to their known proliferative nature and for the presence of landmarks in the tissue (the muscles of the CF in the APC and dorsal artery in the HPT) that allow approximate standardization of the location of these sampling sites. A 4 μm stack composed of 1.0 μm thick images was taken at each location and rendered as a maximum projection in 2D for analysis.

After all imaging was complete, the maximized, 2D stacked images of each APC and HPT region were transferred to a laboratory computer, all images were given a code to hide their identity, and the number of PI-labeled cells and the number of BrdU-labeled cells were counted independently (Figure 1B and 1C). To make these counts, a transparency was taped to the computer screen and each cell was circled by hand and counted. To obtain a percentage of BrdU-labeled cells for each tissue region, the number of BrdU-labeled cells was divided by the total number of PI-labeled cells for each image. For analysis, the four regions sampled in each APC in one animal were averaged and counted as one "n"; likewise, the two regions

sampled from the HPT in one animal were averaged and each animal was counted as a single "n". Due to methodological constraints, at times not all four regions of each APC and both regions of the HPT were available for counting. Thus, some averages represent fewer than the maximum number of counts. However, given the relatively small variability in these counts, these samples were included in the data set.

AST1 injection and BrdU labeling of HPT, APC and niche cells (Figures 2 and 3)

Simultaneous AST1 and BrdU injection of crayfish

Recombinant-AST1 (r-AST1) was generated in the laboratory of Irene Söderhäll (Uppsala University, Sweden) using an *Escherichia coli* expression system, as described in Lin et al., 2010. BrdU (as above) and r-AST1 (Trx-S tag-AST1; 0.05 μg/g animal weight) were injected simultaneously into the ventral hemolymph sinus in the abdomen of crayfish at 09:30 on 'Day 0'.

At various intervals between days 1 and 21 following BrdU or BrdU/r-AST-1 injection, groups of crayfish were sacrificed, brains dissected and desheathed, and processed immunocytochemically for BrdU (as above) and mouse anti-glutamine synthetase (BD Biosciences), followed by nucleic acid labeling with PI. Brains were mounted, viewed and images collected using a Leica TCS SP5 confocal microscope. A niche cell was considered BrdU-labeled if its PI-labeled nucleus also fluoresced at 488 nm (indicating BrdU incorporation). In addition, the cytoplasm of all niche cells labels immunocytochemically for GS. Therefore, for a BrdU-labeled cell to be counted as "in the niche", it had to be GS-labeled and the cell had to be surrounded by other GS-labeled cells, indicating that the cell was in the same plane as other niche cells. For analysis, the percent chance of finding a BrdU-labeled cell in the niche was determined by dividing the number of niches containing at least one BrdU-labeled cell by the total number of niches counted for a single time period.

In vitro and *in vivo* BrdU labeling of hemocytes (Figure 4)

In vitro hemocyte labeling

Hemolymph was collected from adult crayfish (30-35 mm CL) at 8 AM using a 25 gauge 5/8" ice-cold needle coated with AC buffer. Hemolymph was drawn from the dorsal sinus directly into a 1 mL syringe containing AC buffer, to a final ratio of 1 part hemolymph:2 parts AC buffer. The syringe contents were transferred to a sterile Eppendorf tube and gently mixed, and then left undisturbed for 30 min at room temperature to allow cells to settle to the bottom of the tube. After this rest period, supernatant was removed and discarded, leaving 50 μL in the bottom of the tube. This hemolymph sample was then transferred onto a poly L-lysine coated coverslip (Neuvitro Corporation, GG-12-PLL) placed in the well of a culture dish, which was then covered; cells were allowed to adhere for 30 minutes at room temperature. The coverslip with attached cells was then washed with three quick rinses in L-15 medium (Sigma-Aldrich, L5520), which was then replaced with BrdU in L-15 medium (0.5 mg/mL). The dish was then covered and placed in an incubator at 18 °C for 6 hours. The coverslip was then removed from the BrdU and placed in a glass dish. Cells were rinsed in saline (2 x 5 min), followed by 10 min in 4% paraformaldehyde fixative. After three rinses in phosphate buffered saline (PBS) on a rotating platform, the coverslip was allowed to dry overnight.

The next day, the coverslip with attached cells was placed in a clean glass well dish, rinsed with PBTx (6 x 10 min), treated for 15 minutes with 2N HCl and rinsed again in PBS (6 x 10 min). Cells were then incubated overnight in rat anti-BrdU conjugated to Alexa 555 (1:100 in PBTx; Abcam, #ab221240). After PBS rinses (8 x 5 min), the coverslip with attached cells was mounted on a slide with Fluorogel (Electron Microscopy Sciences). Cells and labeling were then visualized and images collected using a Leica TCS SP5 confocal microscope.

In vivo hemocyte labeling

Adult crayfish (30-35 mm CL) were injected with the S-phase marker BrdU (2 mg/mL; 20 μL/gm body weight) at 8AM, and then returned to holding tanks in the Animal Care Facility. For each time point — 6 hours and 7 days post-BrdU injection — hemolymph was collected as described above for *in vitro* studies, to a final ratio of 1 part hemolymph:1 part AC buffer. The contents of the syringe were then transferred to a sterile Eppendorf tube and gently mixed. Immediately thereafter, 100 μL of the hemolymph sample was transferred onto a slide precoated with poly L-lysine. Cells were allowed to adhere for 30 minutes before being rinsed with saline (2 x 5 min) and then fixed with 4% paraformaldehyde (1 x 10 min). After three rinses in phosphate buffered saline (PBS), the slides were left to dry overnight.

The next day, slides were rinsed with PBTx (6 x 10 min), treated for 15 minutes with 2N HCl and rinsed again in PBTx. Cells were then incubated overnight in rat anti-BrdU conjugated to Alexa 555 (1:100 in PBTx; Abcam, #ab221240). The next day, slides were washed with PBTx (6 x 10 min), incubated in DAPI for 2 min (1 μg/ml in PBTx; ThermoFisher Cat #62248), and rinsed with PBS (5 x 5 min). A glass coverslip was then mounted on each slide with FluoroGel (Electron Microscopy Sciences). Cells and labeling were visualized and images collected using a Leica TCS SP5 confocal microscope.

Adoptive transfers of hemocytes (Figures 5, 6, 7, and 8)

Hemolymph labeling and collection

Donor crayfish (30-40 mm CL) for hemolymph were injected with EdU (100 μL of 0.1 mg/mL crayfish saline) and returned to artificial pond water for 7-8 days. On the day of the experiment, hemolymph was collected using a 25-gauge 5/8" cold needle inserted shallowly beneath the ventral abdominal membrane, to the left or right of the abdominal artery, and allowed to bleed directly into an Eppendorf tube filled with cold AC buffer. A 1:2 solution of hemolymph and AC buffer reduced agglutination during pipetting.

Density gradient hemocyte separations

The blood/AC buffer solution was placed on top of a continuous density gradient gel using Percoll Plus (GE Healthcare) that had been prepared according to the method of Söderhäll and Smith, 1983. To prepare the gels, Percoll Plus was diluted to 70% in 0.15 M NaCl solution and then centrifuged at 15,000 g (Sorvall RC 5B; 25 minutes at 4° C) to form the gradient.

One mL of blood/AC buffer solution (1:1 dilution) was gently layered onto the Percoll gradient, which was then centrifuged at 1500 g. Layers 1 and 2 were removed separately and each was combined with 200 μL of filtered crayfish saline, then gently pipetted to re-suspend cells. Hemocytes in each band were examined by mounting cells on slides and viewing with a compound microscope, confirming that each band contained distinct cell types.

Adoptive transfer of specific hemocyte types: granular and semigranular cells (Figures 5 and 6)

Hemocytes extracted from each layer on the gel were injected into separate recipient crayfish. Removal of the Percoll Plus from separated cells was not necessary because this medium has low toxicity, osmolality, and viscosity, and is compatible with living cells; transfers did not cause any noticeable adverse effects in the crayfish. Recipient crayfish were sacrificed 3 days, 7 days, 3 weeks or 6 weeks after transfer of hemocytes from each band on the Percoll gel. Brains and associated niches were processed using the Alexa 488 Click-iT™ reaction cocktail and labeled immunocytochemically for GS (1:100 mouse anti-glutamine synthetase, BD BioSciences, followed by anti-mouse IgG DyLight 649, Jackson Immunoresearch Labs). After staining with the nucleic acid marker Hoechst 33342 (5 μg/mL), brains were mounted with Fluorogel. Brains in the 3- and 6-week transfers were also labeled immunocytochemically for the peptide transmitter SIFamide using a rabbit anti-SIFamide antibody (1:5000; gift of Dr. A Yasuda, Suntory Institute for Bioorganic Research) followed by Cy5-conjugated goat anti-rabbit IgG antibody.

Injections with 5-HT and measurement of total hemocyte counts (THC) (Figure 7A)

Total hemocyte counts (THC) and 5-HT injections

Crayfish for these studies were obtained from Carolina Biological Supply Company (Burlington, NC). Body weight (10-20 gm; 20-35 mm CL) and sex were recorded for each crayfish. Due to large biological variability in THC among crayfish, hemolymph was collected prior to the 5-HT injection in order to acquire a baseline THC. After being left to rest in bins for 24 hours, animals were injected with 5-HT. Post-injection THCs were then determined at intervals (10, 20, 40 and 60 minutes) after 5-HT injection. Percent change in hemocyte counts relative to the baseline THC was then calculated.

For 5-HT injections, serotonin creatinine sulfate (Millipore Sigma, Cat. #H7752) dissolved in crayfish saline was injected into the thoracic cavity of crayfish (100 μl of 50 nM serotonin creatinine sulfate). Based on data published by Rhodes (1982) comparing crayfish blood volumes to body weight in *Austropotamobius pallipes*, a closely related astacid crayfish, the animals used in these experiments had blood volumes ranging from ~0.5 mL-2.5 mL. We therefore calculated that the effective concentration of 5-HT in crayfish plasma

would be approximately 5 nM. To account for the effect of injecting 5-HT, sham control crayfish were injected with 100 μL of crayfish saline.

To obtain blood samples for THC, a 25-gauge 5/8" ice-cold needle was inserted ventrally into the abdomen, to the left or right of the abdominal artery. The needle was gently removed when 30-40 μl of blood was collected in the hub of the needle. For each sample, 10 μl of the collected blood was immediately pipetted into an Eppendorf tube on ice containing 20 μl of AC buffer (1:2 dilution) in order to prevent blood clotting. The blood/AC buffer solution (6 μl) was then mixed with 6 μl of trypan blue (1:1 dilution; ThermoFisher) in order to label dead cells. The resulting solution was pipetted into a disposable 4-chip hemocytometer (Bulldog Bio, Inc.) to determine THC.

Serotonin modulation of niche cell numbers after adoptive transfer of labeled donor cells (Figure 7B inset)

Crayfish (16-20 mm CL) were injected with blood from donors using the same protocol described in Benton et al., 2014. After two days in artificial pond water, half of the recipient crayfish were placed in a 5-HT bath at 10^{-9} M in pond water for 24 hours at 18°C, and then put back in pond water. The other crayfish, which were maintained in pond water throughout this period, served as controls. Animals were sacrificed 3 days after the beginning of 5-HT treatment. The niche cells of recipient crayfish were labeled with Hoechst, and counted by projecting single optical sections of a stack of images onto the monitor. Hoechst-labeled cells were then traced onto a transparent sheet for counting (as in Benton et al., 2011).

Adoptive transfer of hemocytes and 5-HT treatment of recipients (Figures 7B and 8)

Large (40-45 mm CL) crayfish (n=12) were injected with EdU and 7-8 days later, hemolymph was drawn from each crayfish and directly transferred from an individual donor to an individual recipient (n=12, 40-45 mm CL). Hemolymph was collected as described above. Six of these recipients were soaked in 10^{-9} M serotonin creatinine sulfate in pond water for 24 hours on day 3 post-transfer, then returned to pond water; the other 6 recipients were maintained in pond water only (controls). Brains were dissected on day 4 after hemocyte transfer, desheathed, and processed with the Click-iT reaction to reveal sites of EdU incorporation, processed immunocytochemically for GS (as described above), and stained with the nucleic acid marker Hoechst. The number of EdU+ cells in the niche (n=24) and streams was assessed. Image stacks of niches, streams and Clusters 9 and 10 were created using a Leica TCS SP5 confocal microscope. Each niche and its associated stream were examined for the presence of EdU+ cells. EdU-labeled cells were considered to be in the niche if they had cytoplasmic labeling for GS and were surrounded by GS-labeled niche cells that were not labeled with EdU. EdU+ cells were not included in niche cell counts if they were not surrounded by other GS-labeled cells, to ensure that these were actually in the niche, rather than lying on top or beneath.

QUANTIFICATION AND STATISTICAL ANALYSES

Statistical parameters are reported in the figure legends. Data is considered significant if $p<0.05$. Statistical analyses were performed using IBM SPSS Statistics (IBM Corp.) (Figure 7A) and JMP data analysis software (SAS Institute) (Figure 7B).